

# 1 **Intercomparison of bias correction methods for precipitation of** 2 **multiple GCMs across six continents**

3 Young Hoon Song<sup>1</sup>, Eun-Sung Chung<sup>1\*</sup>

4 <sup>1</sup> Faculty of Civil Engineering, Seoul National University of Science and Technology, 232 G  
5 ongneung-ro, Nowon-gu, Seoul 01811, Korea

6  
7 \* Correspondence to: Eun-Sung Chung [eschung@seoultech.ac.kr](mailto:eschung@seoultech.ac.kr)

## 8 9 **Abstract**

10 This study, conducted across six continents, evaluated and compared the effectiveness of three  
11 Quantile Mapping (QM) methods: Quantile Delta Mapping (QDM), Empirical Quantile  
12 Mapping (EQM), and Detrended Quantile Mapping (DQM) for correcting daily precipitation  
13 data from 11 CMIP6 General Circulation Models (GCMs). The performance of corrected  
14 precipitation data was evaluated using ten evaluation metrics, and the Technique for Order of  
15 Preference by Similarity to Ideal Solution (TOPSIS) was applied to calculate performance-  
16 based priorities. Bayesian Model Averaging (BMA) was used to quantify model-specific and  
17 ensemble prediction uncertainties. Subsequently, this study developed a comprehensive index  
18 by aggregating the performance scores from TOPSIS with the uncertainty metrics from BMA.  
19 The results showed that EQM performed the best on all continents, effectively managing  
20 performance and uncertainty. QDM outperformed other methods in specific regions and was  
21 selected more frequently than DQM when greater weight was given to uncertainty. It suggests  
22 that daily precipitation corrected by QDM is more stable than DQM. On the other hand, DQM  
23 effectively reproduces dry climate but shows the highest uncertainty in certain regions,  
24 suggesting potential limitations in capturing long-term climate trends. This study emphasizes  
25 that both performance and uncertainty should be considered when choosing a bias correction  
26 method to increase the reliability of climate predictions.

## 27 28 **Keywords**

29 CMIP6 GCM, Bias correction, Uncertainty, TOPSIS, Comprehensive index

## 31 **1. Introduction**

32           The Coupled Model Intercomparison Project (CMIP) General Circulation Models  
33 (GCMs) have provided critical scientific evidence to explore climate change (IPCC, 2021;  
34 IPCC, 2022). Nevertheless, GCMs exhibit significant biases compared to observational data  
35 for reasons such as incomplete model parameterization and inadequate understanding of key  
36 physical processes (Evin et al., 2024; Zhang et al., 2024; Nair et al., 2023). These deficiencies  
37 with GCM have introduced various uncertainties in climate projections, making ensuring  
38 sufficient reliability in climate change impact assessments difficult. In this context, many  
39 studies have proposed various bias correction methods to reduce the discrepancies between  
40 observational data and GCM simulations, thereby providing more stable results than raw GCM-  
41 based assessments (Cannon et al., 2015; Themeßl et al., 2012; Piani et al., 2010). Despite these  
42 advancements, the suggested bias correction methods differ in their physical approaches,  
43 resulting in discrepancies in the climate variables adjusted for historical periods. Furthermore,  
44 the distribution of precipitation across continents and specific locations causes variations in the  
45 correction outcomes depending on the method used, which makes it challenging to reflect  
46 extreme climate events in future projections and adds another layer of confusion to climate  
47 change research (Song et al., 2022b; Maraëun, 2013; Ehret et al., 2012; Enayati et al., 2021).  
48 Thus, exploring multiple aspects to make reasonable selections when applying bias correction  
49 methods specific to each continent and region is necessary.

50           Many studies have developed appropriate bias correction methods based on various  
51 theories, which have reduced the difference between GCM simulations and observed  
52 precipitation (Abdelmoaty and Papalexiou, 2023; Shanmugam et al., 2024; Rahimi et al., 2021).  
53 Quantile Mapping (QM) series has been widely adopted among bias correction methods due to  
54 its conceptual simplicity, ease of application, and adaptability to various methodologies.  
55 However, although common QM methods have high performance in correcting stationary  
56 precipitation, they are less efficient in non-stationary data, such as extreme precipitation events  
57 (Song et al., 2022b). To address these limitations, a recent study proposed an improved QM  
58 approach to reflect future non-stationary precipitation across all quantiles of historical  
59 precipitation (Rajulapati and Papalexiou, 2023, Cannon et al., 2015, Cannon, 2018; Song et al.,  
60 2022b). In recent years, climate studies using GCMs have adopted several improved QM  
61 methods that offer higher performance than previous methods to correct historical precipitation  
62 and project it accurately into the future. For example, Song et al. (2022b) performed bias

63 correction on daily historical precipitation over South Korea using distribution transformation  
64 methods they developed and found that the best QM method varied depending on the station.  
65 Additionally, previous studies have reported that QM performance varied by grid and station  
66 (Ishizaki et al., 2022; Chua et al., 2022). From this perspective, these improved QMs may only  
67 guarantee uniform results across some grids and regions. Therefore, to analyze positive  
68 changes in future climate impact assessments, it is essential to select appropriate bias correction  
69 methods based on a robust framework.

70 Multi-criteria decision analysis (MCDA) is efficient for prioritization because it can  
71 aggregate diverse information from various alternatives. MCDA has been extensively used  
72 across different fields to select suitable alternatives, with numerous studies confirming its  
73 stability in priority selection (Chae et al., 2022; Chung and Kim, 2014; Song et al., 2024a).  
74 Moreover, MCDA has been employed in future climate change studies to provide reasonable  
75 solutions to emerging problems, including the selection of bias correction methods for specific  
76 regions and countries (Homsy et al., 2019; Saranya and Vinish, 2021). However, MCDA's  
77 effectiveness is sensitive to the source and quality of alternatives, making accurate ranking  
78 challenging when information is lacking or overly focused on specific criteria (Song and Chung,  
79 2016). Small-scale regional and observation-based studies have conducted GCM performance  
80 evaluations, but global and continental-scale evaluations are rare due to the substantial time  
81 and cost required.

82 GCM simulation includes uncertainties from various sources, such as model structure,  
83 initial condition, boundary condition, and parameters (Pathak et al., 2023; Cox and Stephenson,  
84 2007; Yip et al., 2011; Woldemeskel et al., 2014). The selection of bias correction methods  
85 contributes significantly to uncertainty in climate change research using GCMs. Jobst et al.  
86 (2018) argued that GHG emission scenarios, bias correction methods, and GCMs are primary  
87 sources of uncertainty in climate change assessments across various fields. The extensive  
88 uncertainties in GCMs complicate the efficient establishment of adaptation and mitigation  
89 policies. This issue has led to the increased awareness of the uncertainties inherent in historical  
90 simulations. Consequently, many studies have focused on estimating uncertainties using  
91 diverse methods to quantify these uncertainties (Giorgi and Mearns, 2002; Song et al., 2022a,  
92 Song et al., 2023). Although it is impossible to drastically reduce the uncertainty of GCM  
93 outputs due to the unpredictable nature of climate phenomena, uncertainties in GCM  
94 simulations can be reduced using ensemble principles, such as multi-model ensemble

95 development using rational approach (Song et al., 2024). However, accurately identifying  
96 biases in simulation precipitation remains challenging due to the lack of comprehensive  
97 equations reflecting Earth's physical processes. In this context, climate change studies have  
98 aimed to quantify the uncertainty of historical climate variables in GCMs, offering insights into  
99 the variability of GCM simulations (Pathak et al., 2023). Bias-corrected precipitation of GCMs  
100 using QM has shown high performance in the historical period, which is expected to result in  
101 better future predictions. However, the physical concepts of various QMs may lead to more  
102 significant uncertainty in the future (Lafferty et al., 2023). Therefore, efforts should be made  
103 to consider and reduce uncertainty in the GCM selection process. It will ensure the reliability  
104 of predictions by selecting an appropriate bias-correcting method.

105 This study aims to compare the performance of three bias correction methods using  
106 daily historical precipitation data (1980-2014) from CMIP6 GCMs across six continents (South  
107 America: SA; North America: NA; Africa: AF; Europe: EU; Asia: AS; and Oceania: OA). Ten  
108 evaluation metrics were used to assess the performance of daily precipitation corrected by the  
109 three QM methods for each continent. Subsequently, the Technique for Order of Preference by  
110 Similarity to Ideal Solution (TOPSIS) of MCDA was applied to select an appropriate bias  
111 correction method for each continent. Additionally, the uncertainty in daily precipitation for  
112 historical periods was quantified using Bayesian Model Averaging (BMA). By integrating  
113 performance scores from TOPSIS and uncertainty metrics from BMA, this study developed a  
114 Comprehensive Index (CI), which was then used to select the best bias correction method for  
115 each continent. This comprehensive approach ensures a balanced consideration of both  
116 performance and uncertainty, enhancing understanding of the bias correction process based on  
117 the distribution of daily precipitation across continents.

118

## 119 **2. Datasets and methods**

### 120 **2.1 General Circulation Model**

121 This study used 11 CMIP6 GCM to perform bias correction for daily precipitation in the  
122 historical period. Only daily precipitation was used in performing bias correction in this study  
123 because the natural variability relative to projected anthropogenically forced trends is much  
124 larger for precipitation than for temperature (Deser et al., 2012). Table 1 presents the basic  
125 information, such as model names, resolution, and variant labels. The model resolution of 11

126 CMIP6 GCMs was equally re-gridded to  $1^\circ \times 1^\circ$  using linear interpolation. Furthermore, this  
127 study's ensemble member of CMIP6 GCMs was the first member of realizations (r1).

128

129 Table 1. Information of CMIP6 GCMs in this study

Models	Resolution	Climate variables	Variant label
ACCESS-CM2	$1.2^\circ \times 1.8^\circ$	Daily precipitation	r1i1p1f1
ACCESS-ESM1-5	$1.2^\circ \times 1.8^\circ$		
BCC-CSM2-MR	$1.1^\circ \times 1.1^\circ$		
CanESM5	$2.8^\circ \times 2.8^\circ$		
CESM2-WACCM	$0.9^\circ \times 1.3^\circ$		
CMCC-CM2-SR5	$\sim 0.9^\circ$		
CMCC-ESM2	$0.9^\circ \times 1.25^\circ$		
EC-Earth3-Veg-LR	$1.0^\circ \times 1.0^\circ$		
GFDL-ESM4	$1.4^\circ \times 1.4^\circ$		
INM-CM4-8	$\sim 0.9^\circ$		
IPSL-CM6A-LR	$1.1^\circ \times 1.1^\circ$		

130

## 131 2.2 Reference data

132 This study utilized ERA5 reanalysis data from the European Center for Medium-Range  
133 Weather Forecasts (ECMWF) as reference data. The model physics of ERA5 reanalysis data  
134 improved as it employed an Integrated Forecasting System based on CY41r2 (Hersbach et al.,  
135 2020). The model resolution selected in this study was  $1.0^\circ \times 1.0^\circ$ , which was provided by the  
136 institution for research availability. The accuracy of assessing GCM simulation is crucial for  
137 replicating the spatial and temporal variability of observed data (Hamed et al., 2023). In this  
138 context, the ERA5 product has been commonly used to reproduce observed precipitation, for  
139 the evaluation of GCMs' performances.

140

## 141 2.3 Quantile mapping

142 This study employed three (Quantile delta mapping, QDM; Detrended quantile mapping, DQM;  
143 Empirical quantile mapping, EQM) QM methods to correct the simulation of CMIP6 GCMs,  
144 and these methods are commonly used in the climate change research based on the climate  
145 models (Switanek et al., 2017). **This study divided the data into a training period (1980-1996)  
146 and a validation period (1997-2014) to correct the historical period's data. This approach  
147 minimizes the influence of uncertainties associated with future projections, allowing the study  
148 to focus on evaluating the intrinsic performance differences of the QM methods.** The  
149 frequency-adaptation technique, as described by Themeßl et al. (2012), was applied to address

150 potential biases and improve the accuracy of the corrections. The corrected precipitation using  
 151 the QM used a cumulative distribution function, as shown in Equation 1, to reduce the  
 152 difference from the reference data.

$$153 \hat{x}_{m,p}(t) = F_{o,h}^{-1}\{F_{m,h}[x_{m,p}(t)]\} \quad (1)$$

154 where,  $\hat{x}_{m,p}(t)$  presents the bias-corrected results.  $F_{o,h}$  represents the cumulative distribution  
 155 function (CDF) of the observed data, and  $F_{m,h}$  presents the CDF of the model data. The  
 156 subscripts  $o$  and  $m$  denote observed and model data, respectively, and the subscript  $h$  denotes  
 157 the historical period.

158 QDM, developed by Cannon et al. (2015), preserves the relative changes ratio of modeled  
 159 precipitation quantiles. In this context, QDM consists of bias correction terms derived from  
 160 observed data and relative change terms obtained from the model. The computation process of  
 161 QDM is carried out as described in Equation (2) to (4).

$$162 \hat{x}_{m,p}(t) = \hat{x}_{o,m,h,p}(t) \cdot \Delta_m(t) \quad (2)$$

$$163 \hat{x}_{o,m,h,p}(t) = F_{o,h}^{-1}\{F_{m,p}^{(t)}[x_{m,p}(t)]\} \quad (3)$$

$$164 \Delta_m(t) = \frac{x_{m,p}(t)}{F_{m,h}^{-1}\{F_{m,p}^{(t)}[x_{m,p}(t)]\}} \quad (4)$$

165 where,  $\hat{x}_{o,m,h,p}(t)$  presents the bias corrected daily precipitation for the historical period, and  
 166  $\Delta_m(t)$  the relative change in the model simulation between the reference period and the target  
 167 period. In addition, the target period is calculated by multiplying the relative change ( $\Delta_m(t)$ )  
 168 at time ( $t$ ) multiplied by the bias-corrected precipitation in the reference period.  $\Delta_m(t)$  is  
 169 defined as  $\widehat{x_{m,p}}(t)$  divided by  $F_{o,h}^{-1}\{F_{m,p}^{(t)}[x_{m,p}(t)]\}$ .  $\Delta_m(t)$  preserving the relative change  
 170 between the reference and target periods. DQM, while more limited compared to QDM,  
 171 integrates additional information regarding the projection of future precipitation. Furthermore,  
 172 climate change signals estimated from DQM tend to be consistent with signals from baseline  
 173 climate models. The computational process of DQM is performed as shown in Equation (5).

$$174 \hat{x}_{m,p} = F_{o,h}^{-1}\left\{F_{m,h}\left[\frac{\bar{x}_{m,h}x_{m,h}(t)}{\bar{x}_{m,p}(t)}\right]\right\} \frac{\bar{x}_{m,p}(t)}{\bar{x}_{m,h}} \quad (5)$$

175 where,  $\bar{x}_{m,h}$  and  $\bar{x}_{m,p}$  represent the long-term modeled averages for the historical reference  
 176 period and the target period, respectively.

177 EQM is a method that corrects the quantiles of the empirical cumulative distribution function  
 178 from a GCM simulation based on a reference precipitation distribution using a corrected

179 transfer function (Dequé, 2007). The calculation process of EQM can be represented as follows  
 180 in Equation (6).

$$181 \hat{x}_{m,p}(t) = F_{o,h}^{-1}(F_{m,h}(x_{m,p}(t))) \quad (6)$$

182 All these QMs can be applied to the historical data correction in this approach. The bias  
 183 correction is performed based on the relative changes between a reference period and a target  
 184 period in the past, ensuring that the relative changes between these periods are preserved in the  
 185 corrected data (Ansari et al., 2023; Tanimu et al., 2024; Cannon et al., 2015).

186

## 187 2.4 Evaluation metrics

188 This study used the ten-evaluation metrics to assess the output performance of three quantile  
 189 mapping methods against the reference data for the validation period (1997-2014). Seven  
 190 evaluation metrics used in this study are as follows: Root Mean Square Error (RMSE), Mean  
 191 Absolute Error (MAE), Coefficient of Determination ( $R^2$ ), Percent bias (Pbias), Nash-Sutcliffe  
 192 Efficiency (NSE), Kling-Gupta efficiency (KGE), Median Absolute Error (MdAE), Mean  
 193 Squared Logarithmic Error (MSLE), Explained Variance Score (EVS), and Jensen-Shannon  
 194 divergence (JS-D). The equations of seven evaluation metrics are presented in Table 2.

195

196 Table 2. Information of the seven-evaluation metrics used in this study

Metrics	Equations	Factors	References
RMSE	$= \sqrt{\frac{1}{n} \sum_{i=1}^n (X_i^{sim} - X_i^{ref})^2}$	$X_i^{ref}$ reference data $X_i^{sim}$ Bias corrected GCM	Galton, 1886
MAE	$= \sum_{i=1}^n  X_i^{sim} - X_i^{ref} $		
$R^2$	$= 1 - \frac{\sum_{i=1}^n (X_i^{sim} - X_i^{ref})^2}{(X_i^{ref} - \bar{X}_i^{ref})^2}$		
Pbias	$= \frac{\sum_{i=1}^n (X_i^{ref} - X_i^{sim})}{\sum_{i=1}^n X_i^{ref}} \times 100$		
NSE	$= 1 - \frac{\sum_{i=1}^n (X_i^{sim} - X_i^{ref})^2}{\sum_{i=1}^n (X_i^{ref} - \bar{X}_i^{ref})^2}$		
			Nash and Sutcliffe, 1970

MdAE	$= \text{median}( X_i^{sim} - X_i^{ref} )$		
MSLE	$= \frac{1}{n} \sum_{i=1}^n (\log(1 + X_i^{sim}) - \log(1 + X_i^{ref}))^2$		
EVS	$= 1 - \frac{\text{Var}(X^{sim} - X^{ref})}{\text{Var}(X^{ref})}$		
KGE	$= 1 - \sqrt{(r - 1)^2 + (\alpha - 1)^2 + (\beta - 1)^2}$	$r$ Pearson product-moment correlation $\alpha$ Variability error $\beta$ : Bias term	Gupta et al. 2009
JS-D	$= \frac{1}{2} D_{KL} \left( P \parallel \frac{P + Q}{2} \right) + \frac{1}{2} D_{KL} \left( Q \parallel \frac{P + Q}{2} \right)$	$P(x)$ : Probability density distribution of reference data $Q(x)$ : Probability density distribution of GCM $D_{KL}$ : KL-D	Lin, 1991

197

198 Ten-evaluation metrics selected in this study assess GCM performance from various  
199 perspectives, including error (RMSE, MAE, MdAE, and MSLE), deviation (Pbias), accuracy ( $R^2$ , NSE), variability (EVS), correlation and overall performance (KGE), and distributional  
200 differences (JSD). These metrics complement each other by offering a comprehensive  
201 evaluation framework. For instance, while NSE evaluates the overall fit of the simulated data  
202 to observations, KGE provides a holistic view by integrating correlation, variability, and bias  
203 into a single efficiency score, and JS-D captures the difference between the distributions of the  
204 reference data and the bias-corrected GCM output.  
205

206

## 207 **2.5 Generalized extreme value**

208 This study used generalized extreme value (GEV) to compare the extreme precipitation  
209 calculated by the bias-corrected GCM at each grid of six continents over the historical period.  
210 The historical precipitation was compared with the distribution of reference data and bias-  
211 corrected GCM above the 95th quantile of the Probability Density Function (PDF) of the GEV



212 distribution (Hosking et al. 1985). In addition, this study compared the distribution differences  
 213 between the reference data based on the GEV distribution and the corrected GCM using JSD.  
 214 GEV distribution is commonly used to confirm extreme values in climate variables. The PDF  
 215 of the GEV distribution is shown in Equation 7, and the parameters of the GEV distribution  
 216 were estimated using L-moment (Hosking, 1990).

$$217 \quad g(x) = \frac{1}{\alpha} \left[ 1 - k \frac{x-\epsilon}{\alpha} \right]^{\frac{1}{k}-1} \exp \left\{ - \left[ 1 - k \frac{x-\epsilon}{\alpha} \right]^{\frac{1}{k}} \right\} \quad (7)$$

218 where,  $k$ ,  $\alpha$ , and  $\epsilon$  represents a shape, scale, and location of the GEV distribution, respectively.  
 219

## 220 **2.6 Bayesian model averaging (BMA)**

221 The BMA is a statistical technique that combines multiple models to provide predictions that  
 222 account for model uncertainty (Hoeting et al., 1999). BMA is used to integrate predictions from  
 223 GCMs to improve the robustness and reliability of the resulting assemblies. The posterior  
 224 probability of each model is calculated based on Bayes' theorem as shown in Equation 8.

$$225 \quad P(M_k | D) = \frac{P(D|M_k)P(M_k)}{\sum_{j=1}^K P(D|M_j)P(M_j)} \quad (8)$$

226 where,  $P(M_k)$  is the prior probability of model  $M_k$ , and  $P(D | M_k)$  is the likelihood of the data  
 227  $D$  given model  $M_k$ ,  $P(M_k | D)$  is the posterior probability of model  $M_k$ . In addition, the BMA  
 228 prediction  $\hat{Q}_{BMA}$  is the weighted average of the predictions from each model as shown in  
 229 Equation 9.

$$230 \quad \hat{Q}_{BMA} = \sum_{k=1}^K P(M_k | D) \hat{Q}_k \quad (9)$$

231 where,  $\hat{Q}_k$  is the prediction from model  $M_k$ . In this study, BMA was used to quantify the model  
 232 uncertainty and ensemble prediction uncertainty for daily precipitation corrected by three QM  
 233 methods (QDM, EQM, and DQM) applied to 11 CMIP6 GCMs, as shown in Equations 10 and  
 234 11.

$$235 \quad \alpha_w^2 = \frac{1}{K} \sum_{k=1}^K (w_k - \bar{w})^2 \quad (10)$$

236 where,  $K$  is the number of models,  $w_k = P(M_k | D)$  is the weight of model  $M_k$ ,  $\bar{w}$  is the mean  
 237 of the weights, given by  $\bar{w} = \frac{1}{K} \sum_{k=1}^K w_k$ . A higher variance in model weights indicates more  
 238 significant prediction differences, implying greater model uncertainty.

$$239 \quad \sigma_{BMA} = \sqrt{\frac{1}{K} \sum_{k=1}^K (\hat{Q}_k - \hat{Q}_{BMA})^2} \quad (11)$$

240  $\sigma_{BMA}$  is standard deviation of the BMA ensemble predictions,  $\hat{Q}_k$  is the prediction from each  
 241 model  $M_k$ ,  $\hat{Q}_{BMA}$  is the weighted average prediction from BMA. This standard deviation  
 242 represents the variability among the ensemble predictions and serves as an indicator of  
 243 uncertainty. A lower standard deviation implies higher consistency among predictions,  
 244 indicating lower uncertainty, while a higher standard deviation suggests greater variability and  
 245 higher uncertainty.

246

## 247 **2.7 TOPSIS**

248 This study used TOPSIS to calculate a rational priority among three QM methods based on the  
 249 outcomes derived from evaluation metrics. Furthermore, the closeness coefficient calculated  
 250 using TOPSIS was used as the performance metric for the CI. Proposed by Hwang and Yoon  
 251 (1981), TOPSIS is a multi-criteria decision-making technique frequently used in water  
 252 resources and climate change research to select alternatives (Song et al., 2024). As described  
 253 in Equation 12 and 13, the proximity of the three QM methods is calculated based on the  
 254 Positive Ideal Solution (PIS) and the Negative Ideal Solution (NIS).

$$255 D_i^+ = \sqrt{\sum_{j=1}^n w_j (f_j^+ - f_{i,j})^2} \quad (12)$$

$$256 D_i^- = \sqrt{\sum_{j=1}^n w_j (f_j^- - f_{i,j})^2} \quad (13)$$

257 where,  $D_i^+$  is the Euclidean distance of each criterion from the PIS, summing the whole criteria  
 258 for an alternative  $f_j^+$ ,  $j$  presents the normalized value for the alternative  $f_j^+$ .  $w_j$  presents weight  
 259 assigned to the criterion  $j$ .  $D_i^-$  is the distance between the alternative  $f_j^-$  and the NIS. The  
 260 relative closeness is calculated as shown in Equation 14. The optimal value is closer to 1 and  
 261 represents a reasonable alternative.

$$262 C_i = \frac{D_i^-}{(D_i^- + D_i^+)} \quad (14)$$

263

## 264 **2.8 Comprehensive index (CI)**

265 This study proposed a CI to select the best QM method by combining performance scores and  
 266 model uncertainty indicators. The CI integrates the performance scores (closeness coefficient)  
 267 derived from the TOPSIS method with the uncertainty quantified using BMA. This approach  
 268 allows for a balanced evaluation that considers both the effectiveness of the QM methods and  
 269 the associated uncertainties. Uncertainty was quantified in two ways. Model-specific weight

270 variance was calculated using the variance of the model weights assigned by BMA,  
271 representing the uncertainty in selecting the appropriate QM. The standard deviation of BMA  
272 ensemble prediction was calculated to capture the spread and, thus, the uncertainty of the  
273 ensemble forecasts. Both the indicators were normalized using min-max scaler to ensure  
274 comparability. Finally, the calculation process of the CI is performed as shown in Equations  
275 15 and 16.

$$276 \quad UI = \frac{V_w + \sigma_e}{2} \quad (15)$$

$$277 \quad CI = \alpha \times C_i - \beta \times UI \quad (16)$$

278 where,  $UI$  represents the uncertainty indicator.  $V_w$  and  $\sigma_e$  represent the normalized weight  
279 variance and the normalized ensemble standard deviation, respectively, calculated using BMA.  
280  $C_i$  represents the closeness coefficient calculated from TOPSIS.  $\alpha$  represents the weight given  
281 to the performance score,  $\beta$  represents the weight given to the uncertainty indicator.  
282 Furthermore, by adjusting the weights  $\alpha$  and  $\beta$ , the study evaluated the QM methods under  
283 different scenarios. Equal weight ( $\alpha = 0.5, \beta = 0.5$ ) balances performance and uncertainty  
284 equally, and the emphasized performance weight ( $\alpha = 0.7, \beta = 0.3$ ) prioritize performance over  
285 uncertainty. The emphasized uncertainty weight ( $\alpha = 0.3, \beta = 0.7$ ) prioritize uncertainty over  
286 performance. The results from the CI provide a holistic evaluation of the QM methods,  
287 considering both their effectiveness in bias correction and the reliability of their predictions.

288

### 289 **3. Result**

#### 290 **3.1 Assessment of bias correction reproducibility across continents**

##### 291 **3.1.1 Comparison of bias correction effects**

292 This study applied three QM methods to correct daily precipitation data from 11 CMIP6 GCMs  
293 across six continents. Figure 1 presents the results of comparing daily precipitation data before  
294 and after bias correction using Taylor diagram. In general, the precipitation corrected by DQM  
295 showed a larger difference from the reference data than other methods. In contrast, EQM  
296 showed better performance overall than DQM, and many models showed results that were  
297 close to the reference data. The precipitation corrected by QDM also showed good performance  
298 in most continents but slightly lower than EQM. Nevertheless, QDM showed clearly better  
299 results than DQM.

300 In terms of correlation coefficients, precipitation corrected by DQM showed relatively high  
301 values between 0.8 and 0.9 but lower than EQM and QDM. The precipitation corrected by

302 EQM showed high agreement with the reference data, recording correlation coefficients above  
303 0.9 in most continents. QDM generally showed similar correlation coefficients to EQM but  
304 slightly lower values than EQM in North America and Asia.

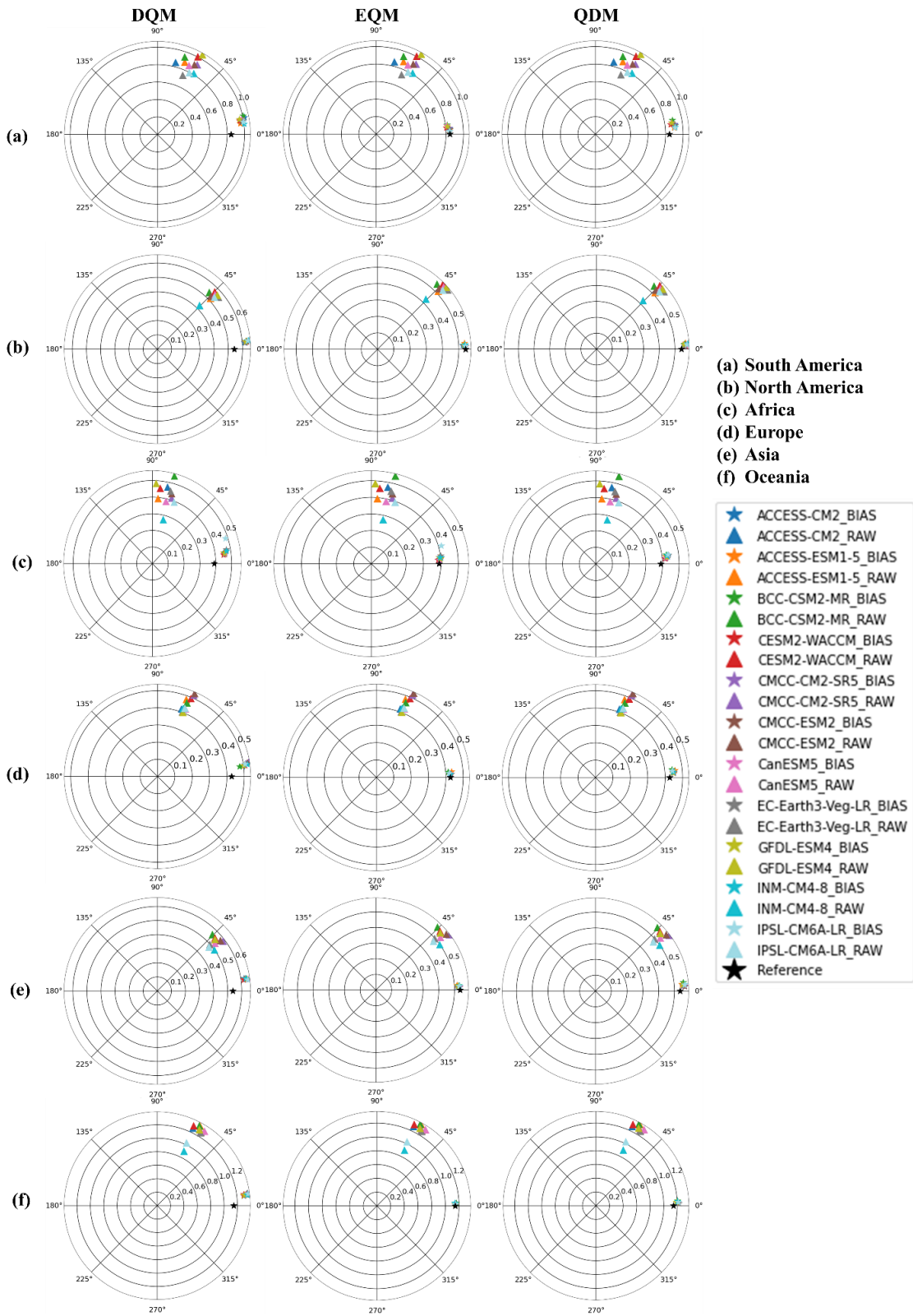
305 For RMSE, precipitation corrected by DQM was higher than EQM and QDM, indicating that  
306 the corrected precipitation differed more from the reference data. On the other hand, EQM had  
307 the lowest RMSE and showed superior performance compared to other methods. QDM had  
308 slightly higher RMSE than EQM but still outperformed DQM.

309 In terms of standard deviation, precipitation corrected by DQM was higher or lower than the  
310 reference data in most continents. On the other hand, precipitation corrected by EQM was  
311 similar to the reference data and almost identical to the reference data in Africa and Asia. QDM  
312 was similar to the reference data in some continents but showed slight differences from EQM.

313 These results imply that the precipitation corrected by the three methods outperforms the raw  
314 simulation, which confirms that the GCM's daily precipitation is reliably corrected in the  
315 historical period.

316

### Taylor diagram



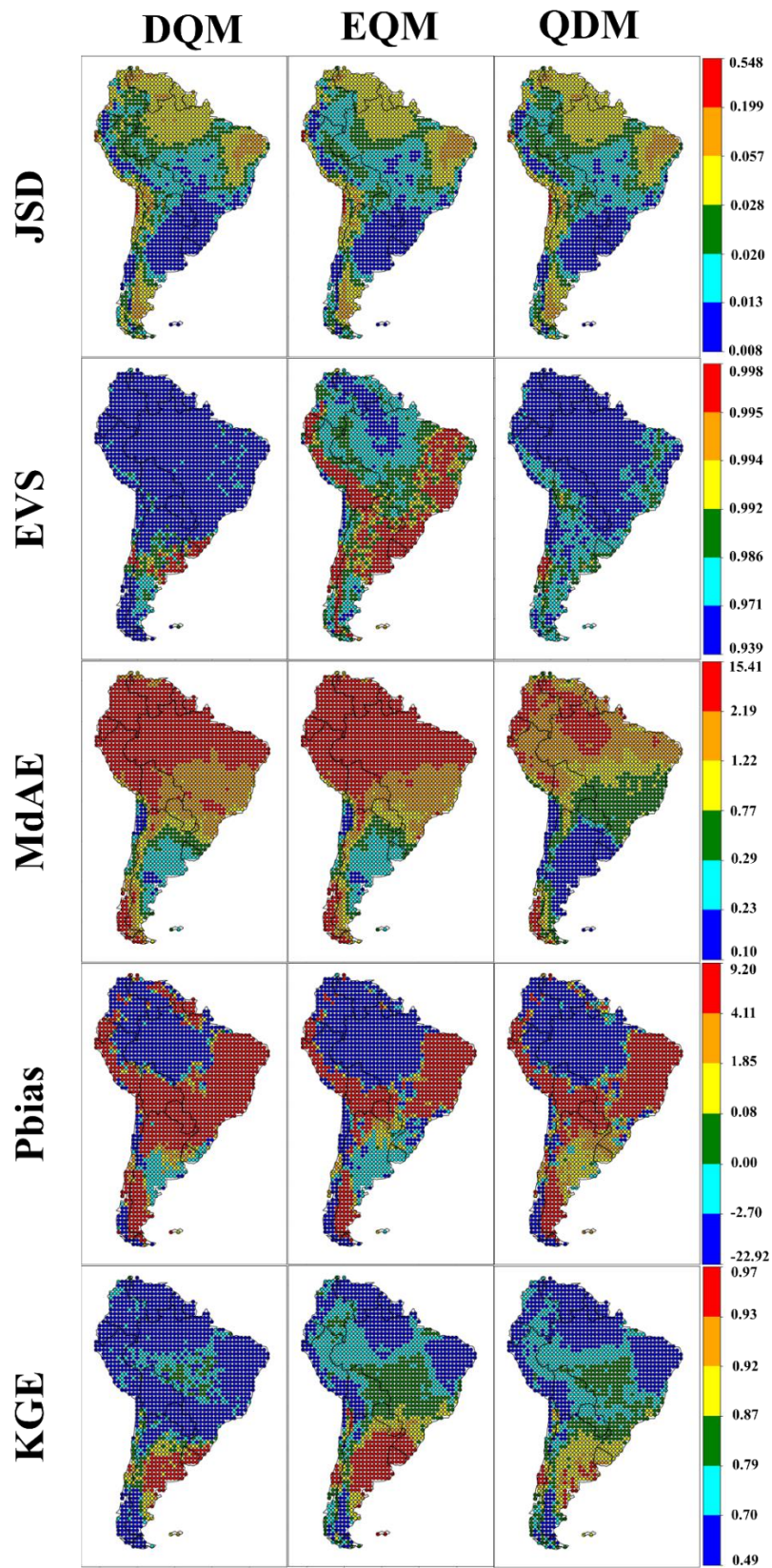
317

318 Figure 1. Comparison of raw and corrected daily precipitation on six continents using Taylor

319 diagrams

### 320 **3.1.2 Spatial distribution of bias correction performance**

321 This study evaluated the performance of daily precipitation across six continents using ten  
322 evaluation metrics for 11 CMIP6 GCMs. Figures 2 and S1 present the spatial patterns of these  
323 evaluation metrics, calculated for daily precipitation from the bias corrected GCMs in South  
324 America. Overall, the precipitation corrected by EQM demonstrated lower JSD values, as well  
325 as higher EVS and KGE values, compared to other methods. The precipitation corrected by  
326 EQM showed higher EVS in certain regions but slightly lower performance in MDAE and Pbias  
327 across some grids. DQM exhibited performance similar to EQM and QDM in most evaluation  
328 indices but was relatively lower in most evaluation metrics. The precipitation corrected by the  
329 three methods was underestimated compared to the reference data in northern South America,  
330 while it was overestimated in eastern South America. In addition, precipitation corrected by  
331 the DQM method tended to be overestimated more than the other methods, while the EQM  
332 method showed the opposite result. Furthermore, the daily precipitation corrected by EQM  
333 showed the lowest overall error and high performance in both NSE and  $R^2$ . QDM and DQM  
334 also performed well but exhibited slightly larger errors in some regions than EQM.  
335



336

337 Figure 2. Performance comparison of DQM, EQM, and QDM using evaluation metrics (JSD,

338 EVS, MdAE, Pbias, and KGE) for daily precipitation in South America.

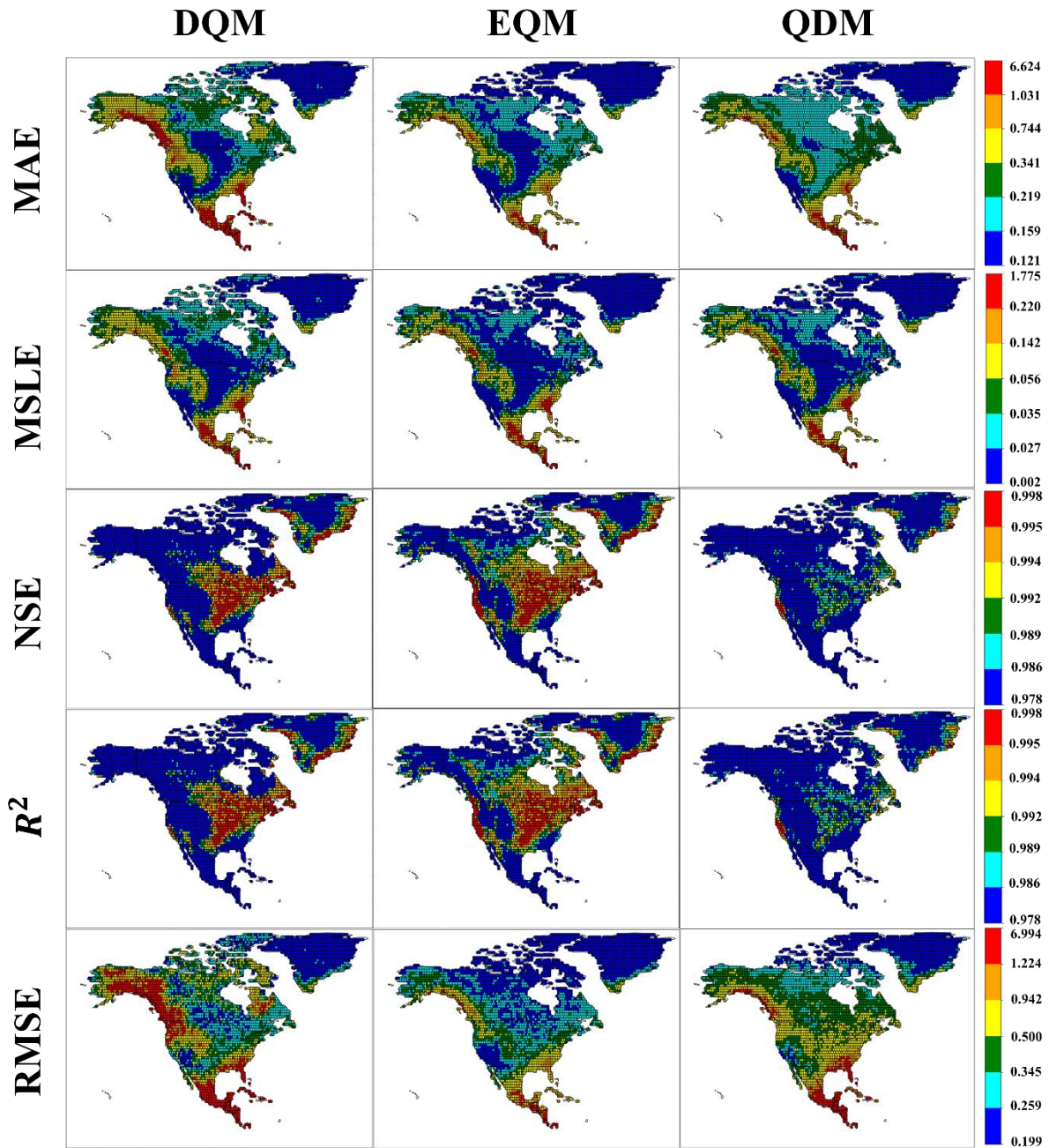
339 Figures 3 and S2 present the spatial patterns of these evaluation metrics, calculated for daily  
340 precipitation from the bias corrected GCMs in South America. Regarding error metrics (MAE,  
341 MSLE, RMSE, and MdAE), precipitation corrected using DQM showed relatively lower  
342 performance across North America, with particularly large errors in the southern region. In  
343 contrast, precipitation corrected using EQM demonstrated superior performance across the  
344 continent compared to other methods. QDM exhibited similar error performance to EQM but  
345 slightly higher errors in the southern region.

346 For correlation metrics (NSE and  $R^2$ ), DQM-corrected precipitation had lower performance  
347 compared to other methods, although there were some grid cells in the central and eastern  
348 regions that exhibited high performance, with values exceeding 0.995. The precipitation  
349 corrected using EQM showed the highest performance, especially in the central and eastern  
350 regions, where most grid points showed correlation coefficients as above 0.995. QDM, while  
351 achieving correlation metrics above 0.978 for most grid points, had slightly lower performance  
352 compared to the other methods.

353 Regarding Pbias, all three methods tended to overestimate precipitation relative to the reference  
354 data across most grid points in North America, while corrected precipitation in Greenland was  
355 underestimated. For JSD, EVS, and KGE metrics, EQM-corrected precipitation showed the  
356 highest performance, with DQM and QDM performing lower than EQM.

357





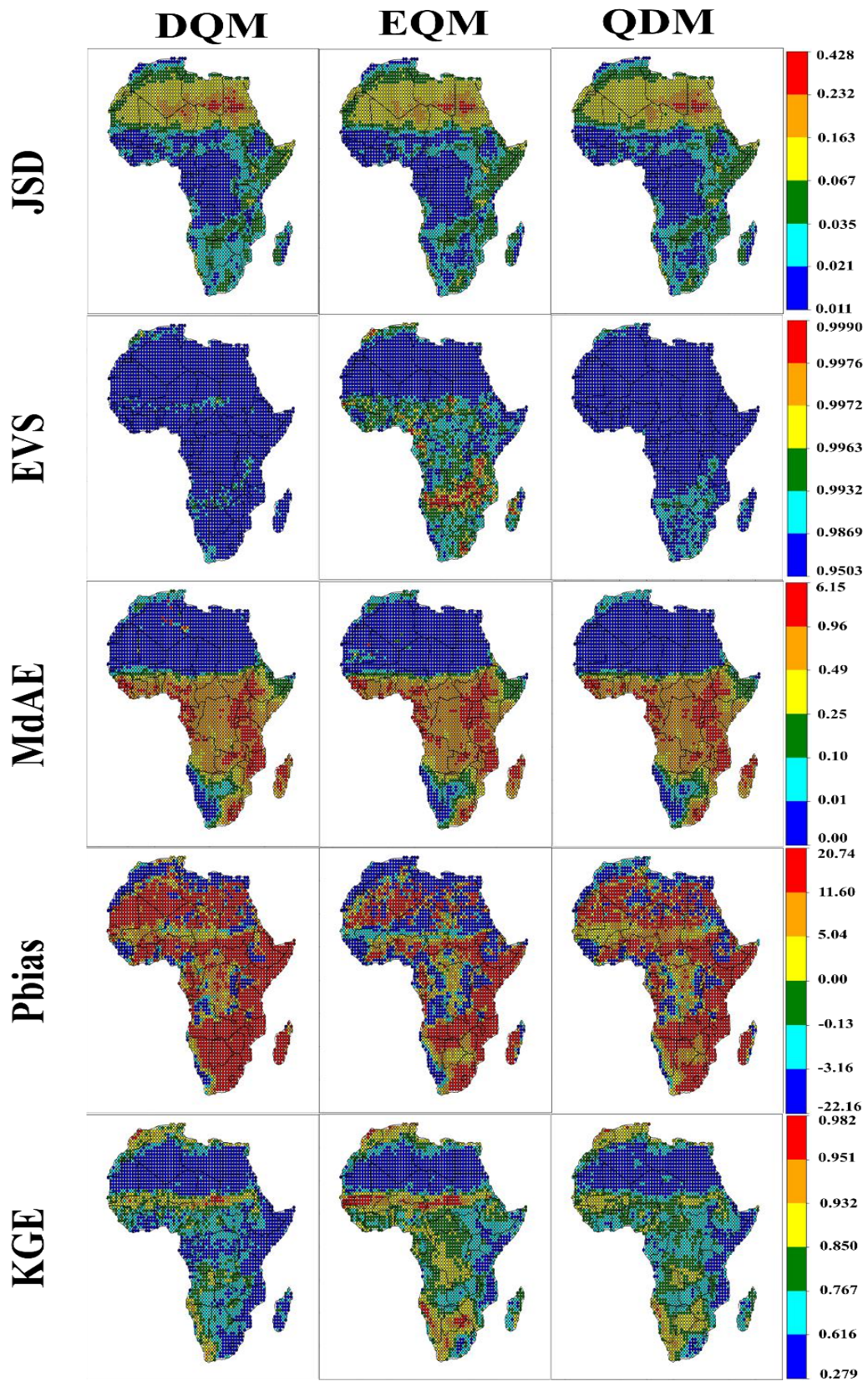
358

359 Figure 3. Performance comparison of DQM, EQM, and QDM using evaluation metrics (MAE,  
 360 MSLE, NSE,  $R^2$ , and RMSE) for daily precipitation in North America.

361

362 In this study, the daily precipitation in Africa was corrected using three QM methods, and the  
 363 performance is shown in Figures 4 and S3. Overall, the JSD of precipitation corrected by the  
 364 three methods showed similar spatial patterns, but the precipitation of DQM showed lower  
 365 performance than the other methods in the southern region. In terms of EVS, the precipitation  
 366 of DQM showed higher variability than the other methods. The precipitation of QDM showed

367 lower variability in southern Africa than DQM, but overall, it showed higher variability than  
368 EQM. The precipitation of EQM showed lower variability in southern and central Africa but  
369 still showed high variability in the northern region. Analyzing the error performance, the  
370 precipitation corrected by QDM showed the best performance compared to the other methods.  
371 In particular, QDM showed the highest performance in North Africa (MAE: 0.03, and MSLE:  
372 0.004), and EQM's error performance was lower than QDM's in most indicators but better than  
373 DQM's. Finally, EQM performed the highest in correlation metrics (NSE and  $R^2$ ), and QDM  
374 performed better than DQM.

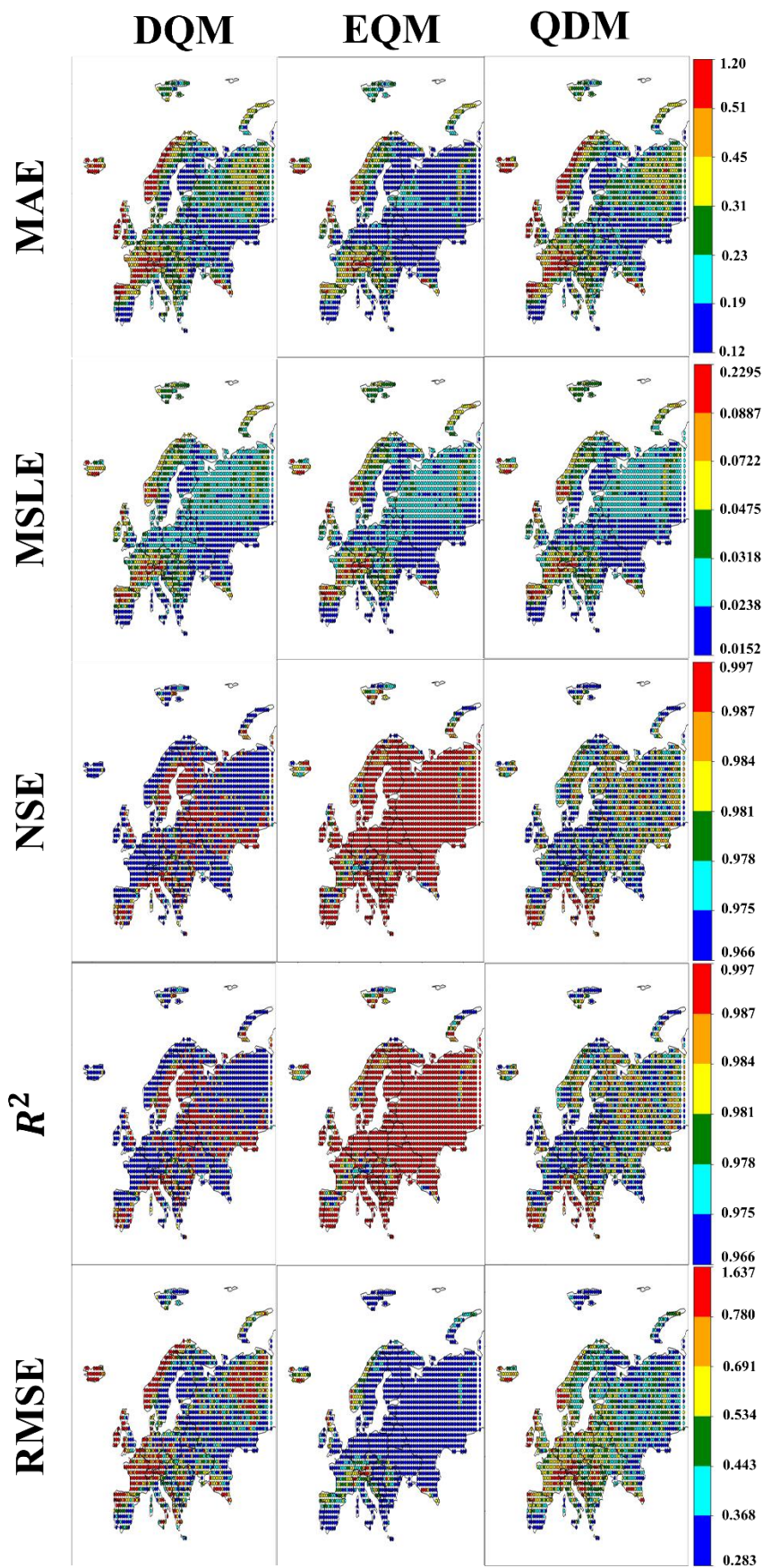


375

376 Figure 4. Performances of DQM, EQM, and QDM using evaluation metrics (JSD, EVS, MdAE,

377 Pbias, and KGE) for daily precipitation in Africa.

378 Figures 5 and S4 show the spatial results of the grid-based evaluation metrics for the European  
379 region. In terms of error metrics, EQM-corrected precipitation performed the best across  
380 Europe compared to other methods. In contrast, QDM-corrected precipitation performed  
381 similarly to DQM in MAE and MSLE but significantly outperformed DQM in RMSE.  
382 Regarding NSE and R, EVS, and KGE metrics, EQM-corrected precipitation performed  
383 overwhelmingly better than other methods. QDM precipitation performed better than DQM,  
384 while DQM performed the worst. Regarding Pbias, EQM-corrected precipitation was  
385 underestimated compared to the reference data in most parts of Europe. In contrast, QDM-  
386 corrected precipitation was more similar to the reference data compared to other methods, and  
387 DQM precipitation was overestimated compared to the reference data except in central Europe.

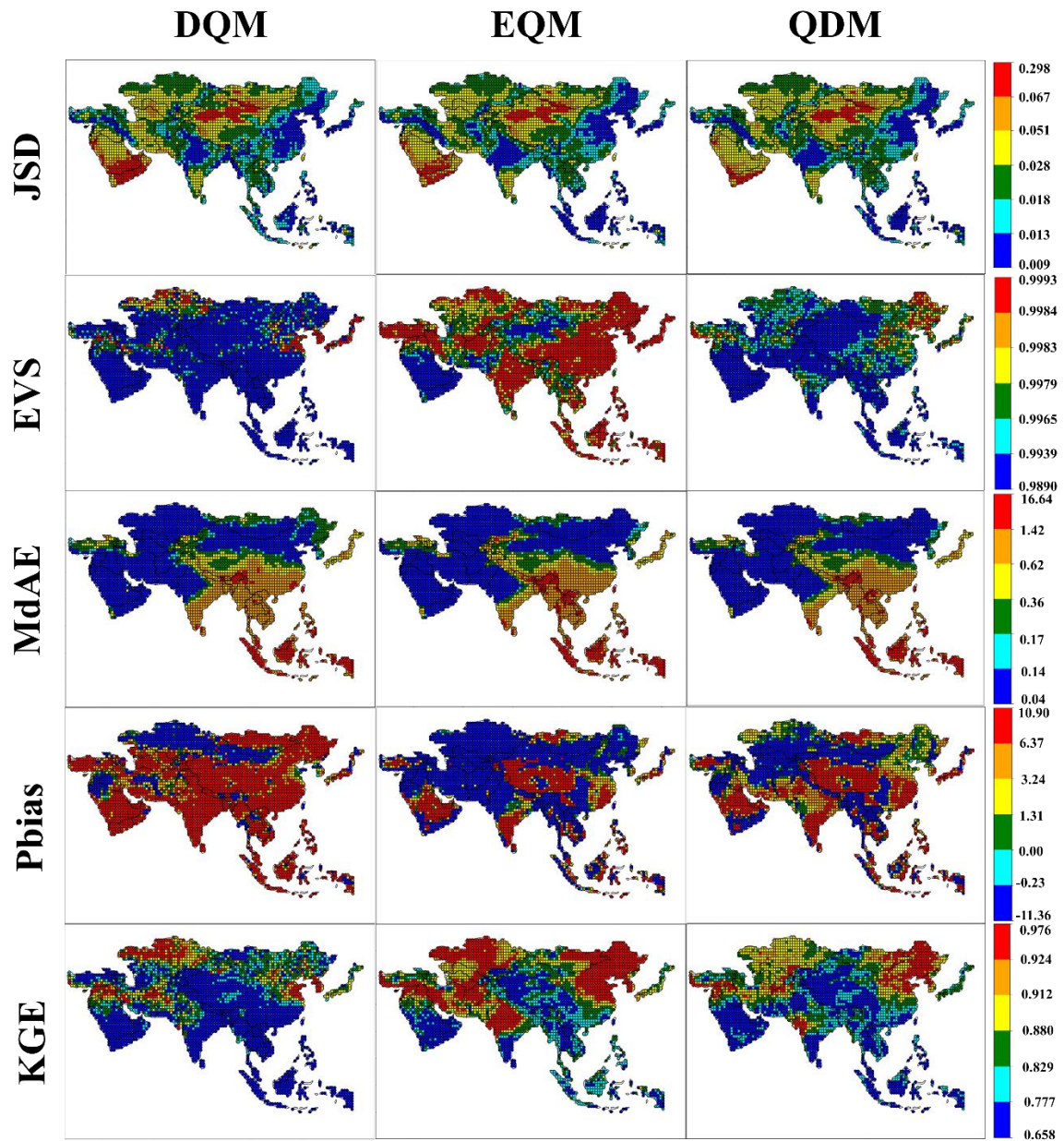


389 Figure 5. Performances of DQM, EQM, and QDM using evaluation metrics (MAE, MSLE,  
390 NSE,  $R^2$ , and RMSE) for daily precipitation in Europe.

391 Figures 6 and S5 show the results of spatially quantifying the corrected precipitation in Asia  
392 using various evaluation metrics. When it comes to error metrics, EQM-corrected precipitation  
393 stands out with its superior performance, particularly in RMSE, which was consistently below  
394 1.35 in most areas of Asia, except for certain parts of Central Asia. In contrast, DQM-corrected  
395 precipitation showed the poorest performance in error metrics. QDM-corrected precipitation  
396 demonstrated a performance similar to EQM, but with a slightly lower performance in East  
397 Asia and North Asia. In NSE and R, the precipitation corrected by EQM performed better than  
398 other methods, especially in Southwest Asia and East Asia. In contrast, the precipitation  
399 corrected by DQM performed lower than other methods. Regarding EVS, the precipitation  
400 corrected by EQM showed the lowest variability, while QDM showed higher variability than  
401 EQM but lower variability than DQM.

402 In the case of Pbias, precipitation corrected by DQM was overestimated compared to the  
403 reference data throughout Asia. The precipitation corrected by EQM was underestimated in  
404 most regions except Central Asia. Precipitation in QDM showed a similar spatial pattern to that  
405 in EQM, but the range of Pbias was more diverse.

406



407

408 Figure 6. Performances of DQM, EQM, and QDM using evaluation metrics (JSD, EVS, MdAE,  
 409 Pbias, and KGE) for daily precipitation in Asia.

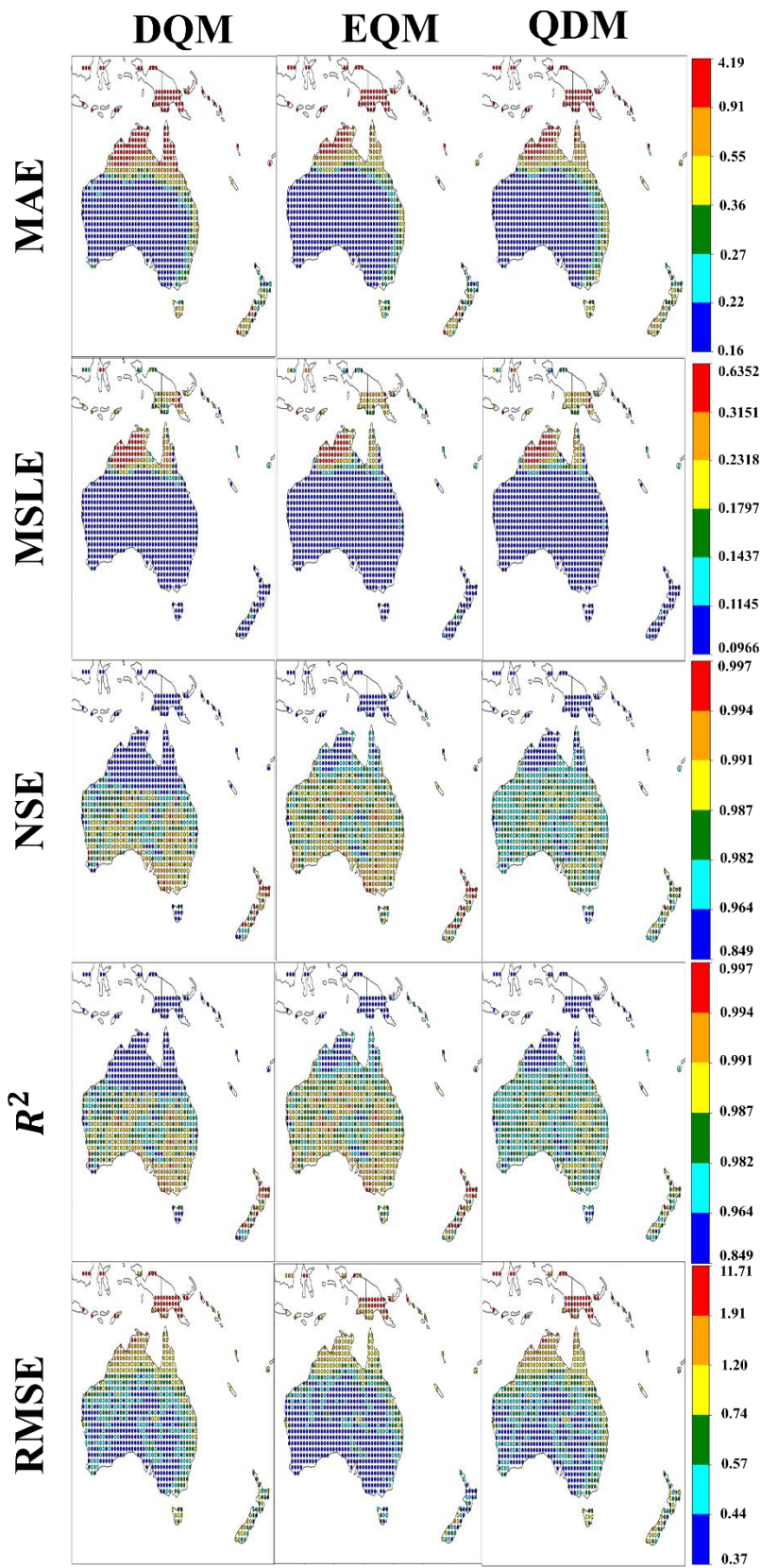
410

411 Figures 7 and S6 show the results of spatially quantifying the corrected daily precipitation in  
 412 Oceania using various evaluation metrics.

413 In terms of error metrics, the precipitation estimated by the three QM methods performed  
 414 similarly in MAE, MdAE, and MSLE. However, the precipitation corrected by EQM  
 415 performed better in RMSE than the other methods. In the case of JSD, all three methods  
 416 performed well.

417 Regarding EVS, the precipitation corrected by EQM showed lower variability than the other  
418 methods, and DQM showed higher performance than QDM. In Pbias, the precipitation adjusted  
419 by QDM was overestimated compared to the reference data in Oceania, while the precipitation  
420 corrected by DQM and EQM was underestimated compared to the reference data in central and  
421 southern Oceania. Finally, in KGE, precipitation corrected by EQM showed the highest  
422 performance, while DQM showed the lowest performance.





423

424 Figure 7. Performances of DQM, EQM, and QDM using evaluation metrics (MAE, MSLE,

425 NSE,  $R^2$ , and RMSE) for daily precipitation in Asia.

426 Figure 8 visualizes the results of evaluating the bias-corrected precipitation data using 11  
427 CMIP6 GCMs on six continents using ten evaluation metrics as boxplots. Overall, the  
428 precipitation corrected by EQM outperforms the other methods on most continents. In  
429 particular, EQM performs the best on the error metrics. QDM performs slightly lower than  
430 EQM but still maintains a high level of performance on all continents. On the other hand, DQM  
431 has larger errors and relatively poor performance compared to the other methods on most  
432 metrics.



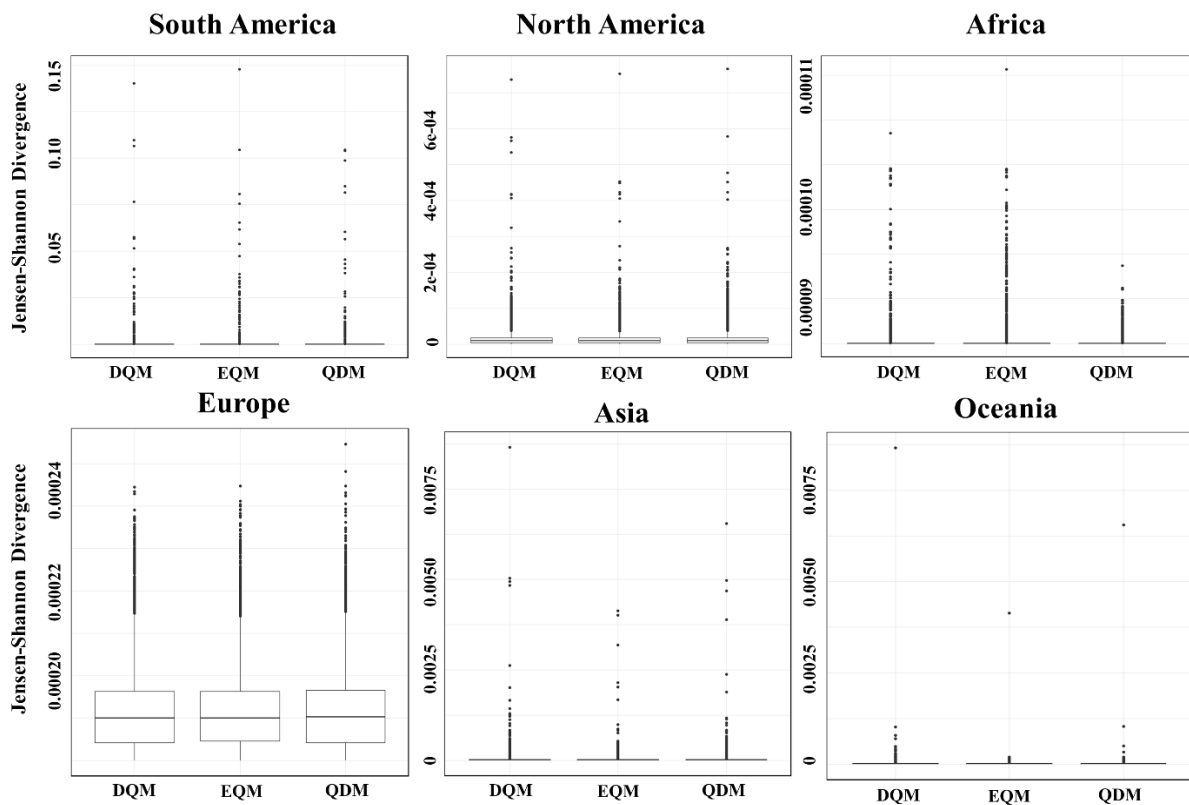
(a) South America (b) North America (c) Africa (d) Europe (e) Asia (f) Oceania

433  
434  
435  
436

Figure 8. Performances of DQM, EQM, and QDM of historical period precipitation using boxplots based on ten evaluation metrics

437 **3.1.3 Comparison of reproducibility for extreme daily precipitation**

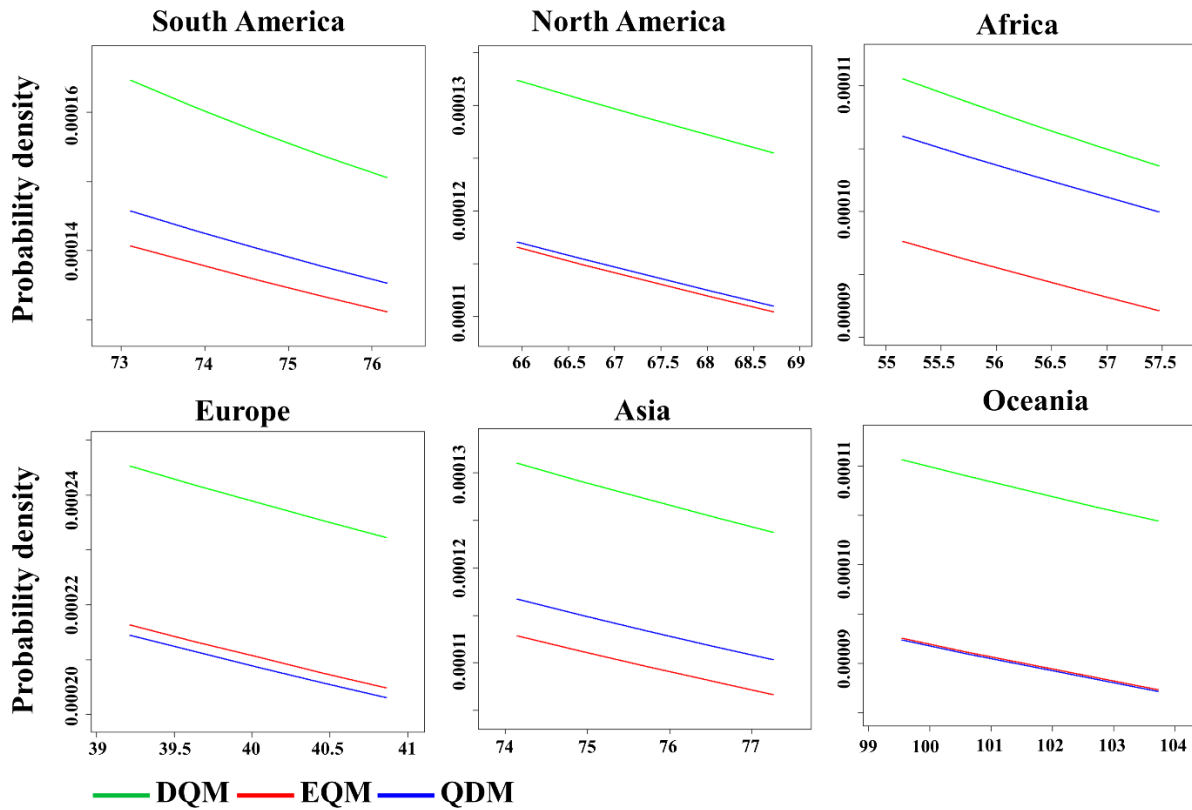
438 This study compared the daily extreme precipitation corrected by three methods using the GEV  
439 distribution. Figure 9 compares the distribution differences of the daily precipitation adjusted  
440 by the biased bias correction methods based on the GEV distribution using the JSD. In general,  
441 the JSD values for precipitation from DQM, EQM, and QDM are very low for most continents,  
442 indicating that the GEV distributions are almost identical among the three methods. Although  
443 there are some outliers, the overall distribution differences are not large, suggesting that there  
444 is little difference among the three methods when correcting for historical precipitation.  
445 However, in Europe, unlike other continents, the differences between the 1st and 3rd quartiles  
446 of the JSD are relatively significant, indicating that the distributions can vary significantly from  
447 grid to grid depending on the QM method.  
448



449 Figure 9. Comparison of distribution differences for GEV distribution using JSD across six  
450 continents.  
451

452  
453 Figure 10 shows the probability density functions for extreme precipitation above the 95th  
454 percentile of the GEV distribution. Overall, DQM shows the highest probability density for

455 extreme precipitation across all continents and has the widest distribution, indicating that DQM  
 456 corrects more extreme precipitation. On the other hand, EQM shows the lowest probability  
 457 density and conservatively corrects for extreme precipitation. QDM shows probability  
 458 densities between those of EQM and DQM across most continents but closer to EQM.



459  
 460 Figure 10. Comparison of probability densities for extreme precipitation values above the 95th  
 461 percentile using GEV.

462

### 463 3.2 Prioritization of bias correction methods based on performance

#### 464 3.2.1 Results of weight for evaluation metrics

465 In this study, the weights were calculated by applying entropy theory to the evaluation metrics  
 466 used in the TOPSIS analysis, and the results are presented in Table 3. Overall, JSD had the  
 467 highest weight in South America because the estimated JSD from 11 CMIP6 GCMs was an  
 468 important metric for evaluating model performance differences. These results indicate that the  
 469 differences between distributions are large. On the other hand, EVS and NSE in South America  
 470 had very low weights, suggesting that the variability and efficiency of precipitation were  
 471 considered less important than other indicators. For North America, the RMSE, MSLE, and  
 472 MAE metrics were of significant importance, as evidenced by their high weights. These error

473 metrics revealed substantial regional differences. In contrast, EVS carried a negligible weight,  
 474 suggesting it was considered less important in explaining variability in North America. For  
 475 Africa, MdAE and JSD metrics were of considerable importance, as indicated by their high  
 476 weights. These metrics were key evaluation factors in Africa. Conversely, EVS carried a low  
 477 weight, suggesting it was considered relatively less important. RMSE had the highest weight  
 478 in Europe, and KGE also had a relatively high weight, indicating that these metrics were  
 479 considered important evaluation criteria in Europe. In Asia, MAE and MSLE had high weights,  
 480 suggesting that these metrics were important evaluation metrics. On the other hand, EVS and  
 481 NSE were considered less important due to their low variability. JSD, KGE, RMSE, and MAE  
 482 were assigned high weights in Oceania, indicating that these metrics are essential factors. On  
 483 the other hand,  $R^2$  and NSE were assigned low weights.

484  
 485 Table 3. Entropy-based weights for evaluation metrics across different continents

	RMS E	MAE	$R^2$	NSE	KGE	Pbias	MdAE	MSLE	EVS	JSD
South America	0.1439	0.1536	0.0001	0.0001	0.0005	0.0238	0.1754	0.1934	0.0004	0.3088
North America	0.2289	0.1908	0.0001	0.0001	0.0007	0.0118	0.2152	0.2117	0.0001	0.1411
Africa	0.1319	0.1686	0.0002	0.0002	0.0002	0.0855	0.2436	0.1911	0.0002	0.1786
Europe	0.2821	0.1762	0.0022	0.0022	0.0063	0.0378	0.1754	0.1666	0.0021	0.1490
Asia	0.2073	0.1954	0.00003	0.00003	0.0001	0.0305	0.2300	0.2024	0.00003	0.1342
Oceania	0.2384	0.2204	0.0013	0.0013	0.0068	0.0214	0.2338	0.2093	0.0012	0.0660

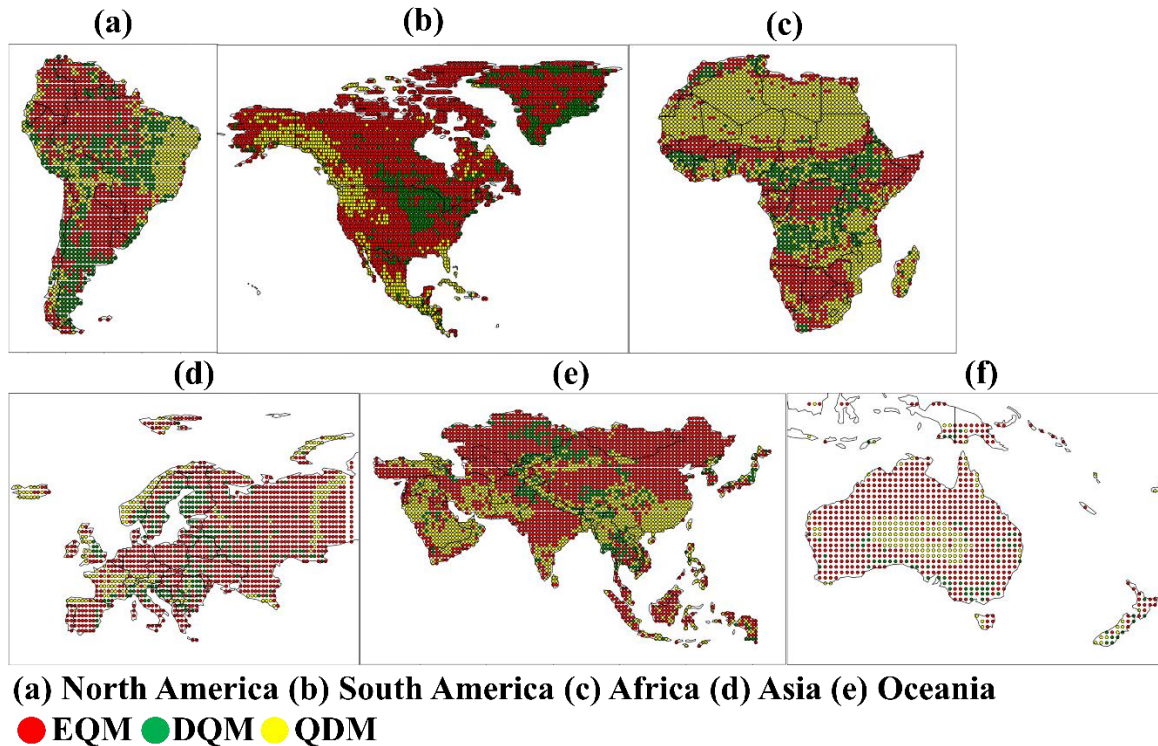
486

487

### 488 3.2.2 Selection of the best bias correction method based on TOPSIS

489 Figure 11 and S7 presents the best bias correction method selected for each continent using the  
 490 TOPSIS approach. In Figure 11(a), the spatial distribution of the most effective bias correction  
 491 method across the grid points of each continent is shown. In contrast, Figure 11(b) shows the  
 492 number of grid points selected for each QM method. In South America, EQM was chosen as  
 493 the best method in most grid points, with EQM being selected in over 1,500 grid points. In  
 494 contrast, QDM was selected in fewer than 700 grid cells, making it the least chosen method in  
 495 South America. Across all continents except South America, EQM was selected as the best  
 496 model in the majority of grid cells, with the number of selected grid points (North America:

497 7,583; Africa: 2,879; Europe: 2,719; Asia: 8,793; and Oceania: 1,659). On the other hand,  
 498 DQM was the least chosen method across all continents. For QDM, although it was the second  
 499 most selected method across all continents except South America, the difference in the number  
 500 of grid points between QDM and EQM is significant.



501  
 502 Figure 11 Spatial distribution for selected best bias correction methods across continents  
 503 using TOPSIS  
 504

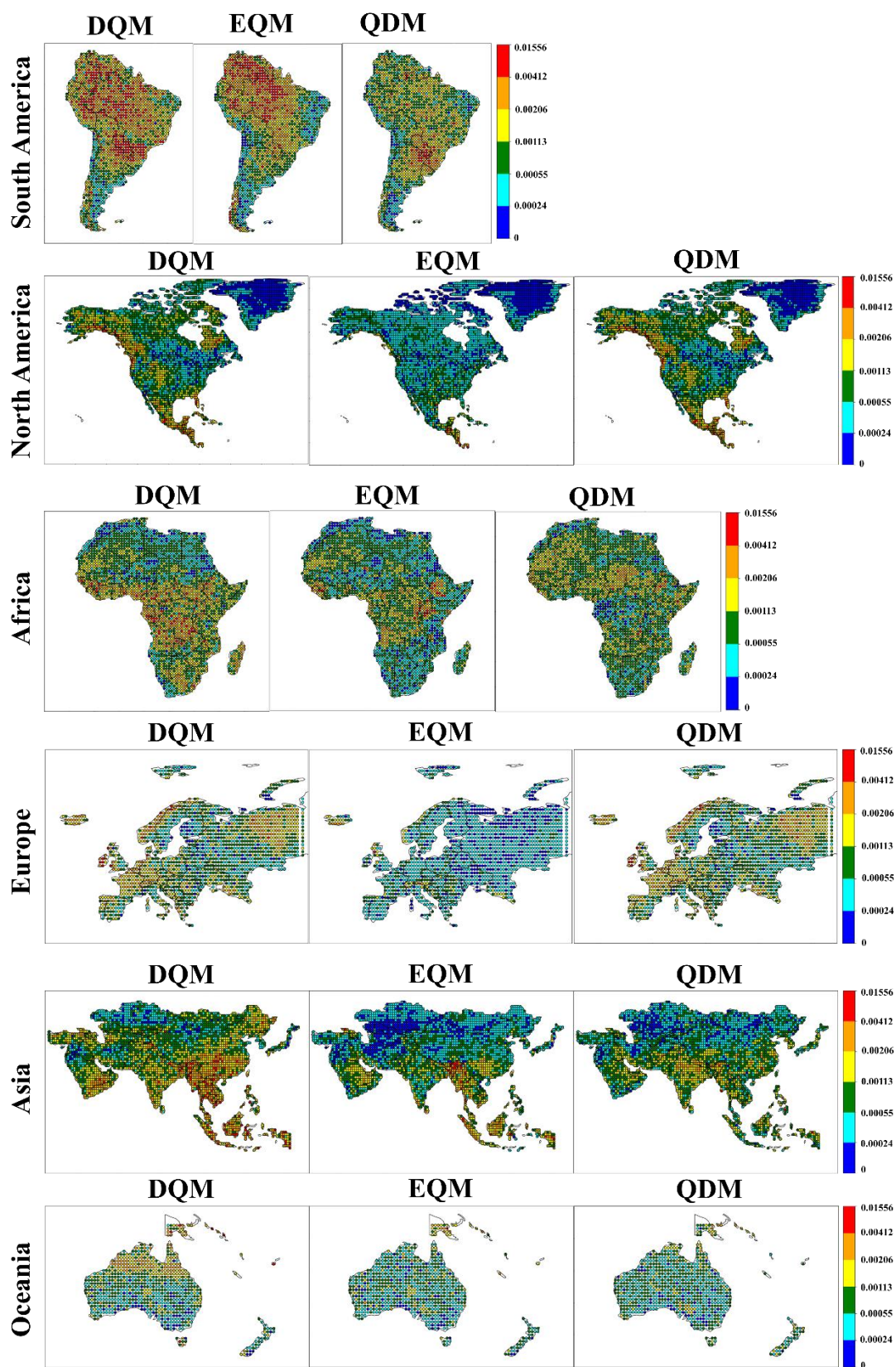
### 505 3.3 Uncertainty quantification of bias corrected daily precipitation

#### 506 3.3.1 Uncertainty by model

507 This study quantifies the daily precipitation uncertainty of 11 CMIP6 GCMs, corrected using  
 508 three different methods, using BMA. Figure 12 shows the distribution of GCM weight  
 509 variances calculated by BMA across six continents. In South America, the highest weight  
 510 variance was observed mainly in DQM. EQM showed high weight variance in the northern  
 511 region but lower variance than DQM in most other regions. QDM exhibited the lowest weight  
 512 variance, with values less than 0.00113 in most regions. In North America, EQM had the lowest  
 513 weight variance, with values between 0.00055 and 0.00024 in most regions. QDM showed the  
 514 lowest model uncertainty across North America, with more regions where weight variances  
 515 were closer to 0 than the other methods. On the other hand, DQM exhibited high weight

516 variance overall, with exceptionally high model uncertainty in the northeast and southern  
517 regions. In Africa, EQM's weight variance was estimated to be low overall, resulting in low  
518 model uncertainty in most regions. For QDM, weight variance was low in some regions, but  
519 higher than 0.00113 in others. DQM showed high weight variance in most regions except for  
520 the northern area, indicating high model uncertainty across the continent. EQM's weight  
521 variance was the lowest in Europe compared to the other methods, with weight variances close  
522 to 0 across the continent. QDM also showed low weight variance overall, though higher than  
523 EQM. DQM exhibited high weight variance in most regions except for Central Europe. In Asia,  
524 EQM showed low weight variance in most regions except Southeast Asia. QDM's weight  
525 variance was similar to EQM's, though some regions had higher model uncertainty. DQM  
526 showed high weight variance in most regions except for some Southwest and North Asian areas.  
527 For Oceania, the weight variances of EQM and DQM were mainly similar, but DQM showed  
528 a higher weight variance overall.



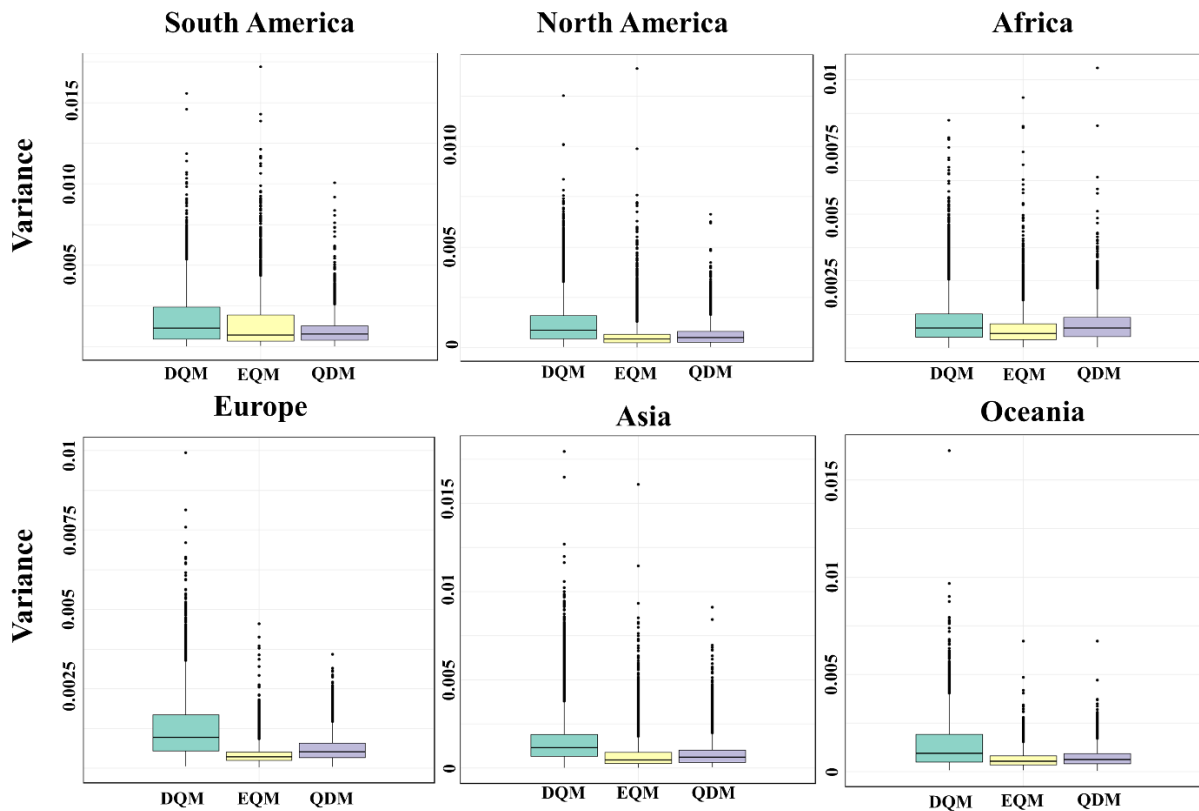


529

530 Figure 12. Spatial distribution of weight variance across continents for bias corrected CMIP6

531 GCMs using BMA

532 Figure 13 shows the distribution of GCM weight variances calculated using BMA across six  
 533 continents, presented as boxplots. Overall, EQM has the smallest weight variance, and QDM  
 534 has the second smallest weight variance on all continents except South America. In contrast,  
 535 in South America, QDM has the smallest weight variance, and EQM has the second smallest.  
 536 DQM consistently has the largest weight variance across all continents, indicating the highest  
 537 model uncertainty.  
 538

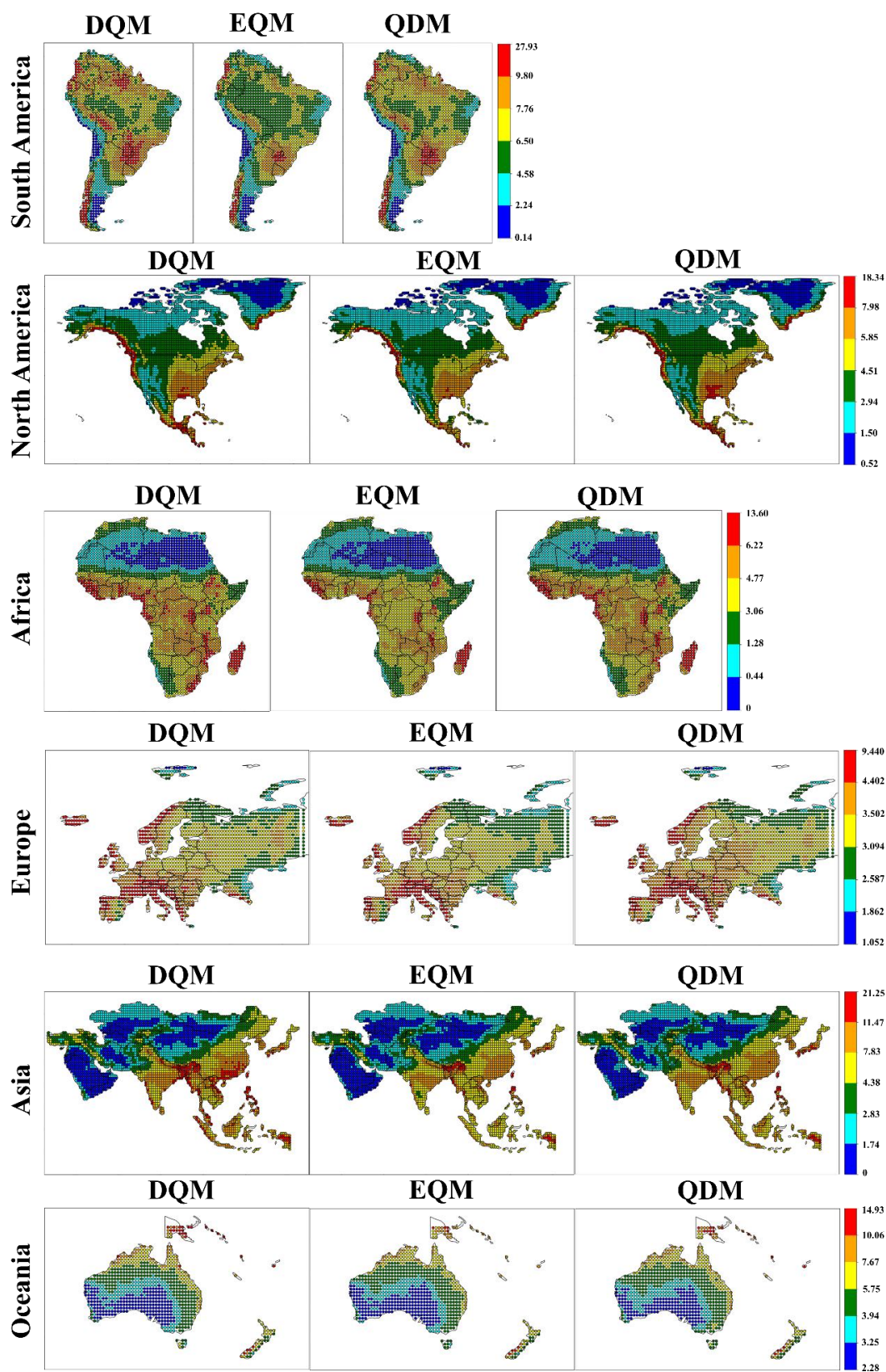


539  
 540 Figure 13. Weight variance for bias correction methods across six continents using box plots.  
 541

### 542 3.3.2 Uncertainty by ensemble prediction

543 This study developed a daily precipitation ensemble for the historical period based on 11  
 544 CMIP6 GCMs using BMA. Figure 14 shows the standard deviation of daily precipitation for  
 545 the historical period by continent for the ensemble developed using BMA with 11 CMIP6  
 546 GCMs. Overall, the ensemble predicted using EQM provided stable precipitation projection  
 547 with low standard deviations across most continents. The QDM ensemble showed similar  
 548 results to EQM for most continents except Oceania, but the standard deviations were slightly  
 549 higher. On the other hand, the ensemble using DQM exhibited higher standard deviations than

550 the other methods for all continents and had the largest prediction uncertainty. In Oceania, the  
551 ensembles predicted by the three methods showed similar results. However, the prediction  
552 uncertainty was estimated to be lower in the order of EQM, DQM, and QDM due to slight  
553 differences.



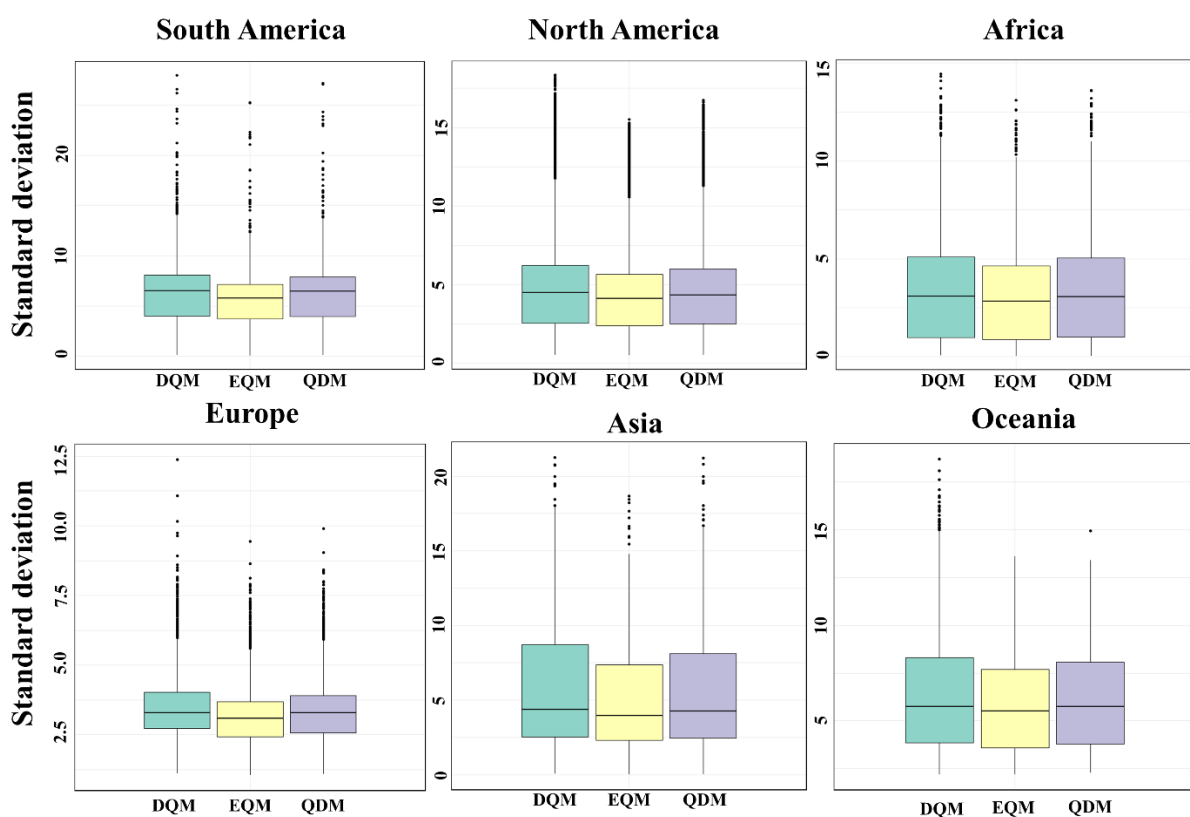
554

555 Figure 14. Spatial distribution of standard deviation for daily precipitation across continents

556 for bias corrected CMIP6 GCMs using BMA

557  
558  
559  
560  
561  
562  
563  
564  
565

Figure 15 shows the standard deviation of daily precipitation for the ensemble forecasted by BMA using three methods, DQM, EQM, and QDM, in a boxplot for each continent. Overall, the EQM ensemble showed the lowest standard deviation across all continents, providing the most stable daily precipitation forecasts. The QDM ensemble showed slightly higher standard deviations than EQM for most continents, but there was no significant difference between the two methods. In contrast, the ensemble using DQM showed the highest standard deviation and the largest prediction uncertainty.



566  
567  
568  
569

Figure 15. Spatial distribution of standard deviation for daily precipitation across continents for bias corrected CMIP6 GCMs using BMA

### 570 3.4 Evaluation of bias correction methods using CI

#### 571 3.4.1 Results of CI by each weighting case

572 This study compared three QM methods by generating a CI based on three cases of weighting  
573 values that considered both model performance and uncertainty. Figures 16, S8, and S9 show

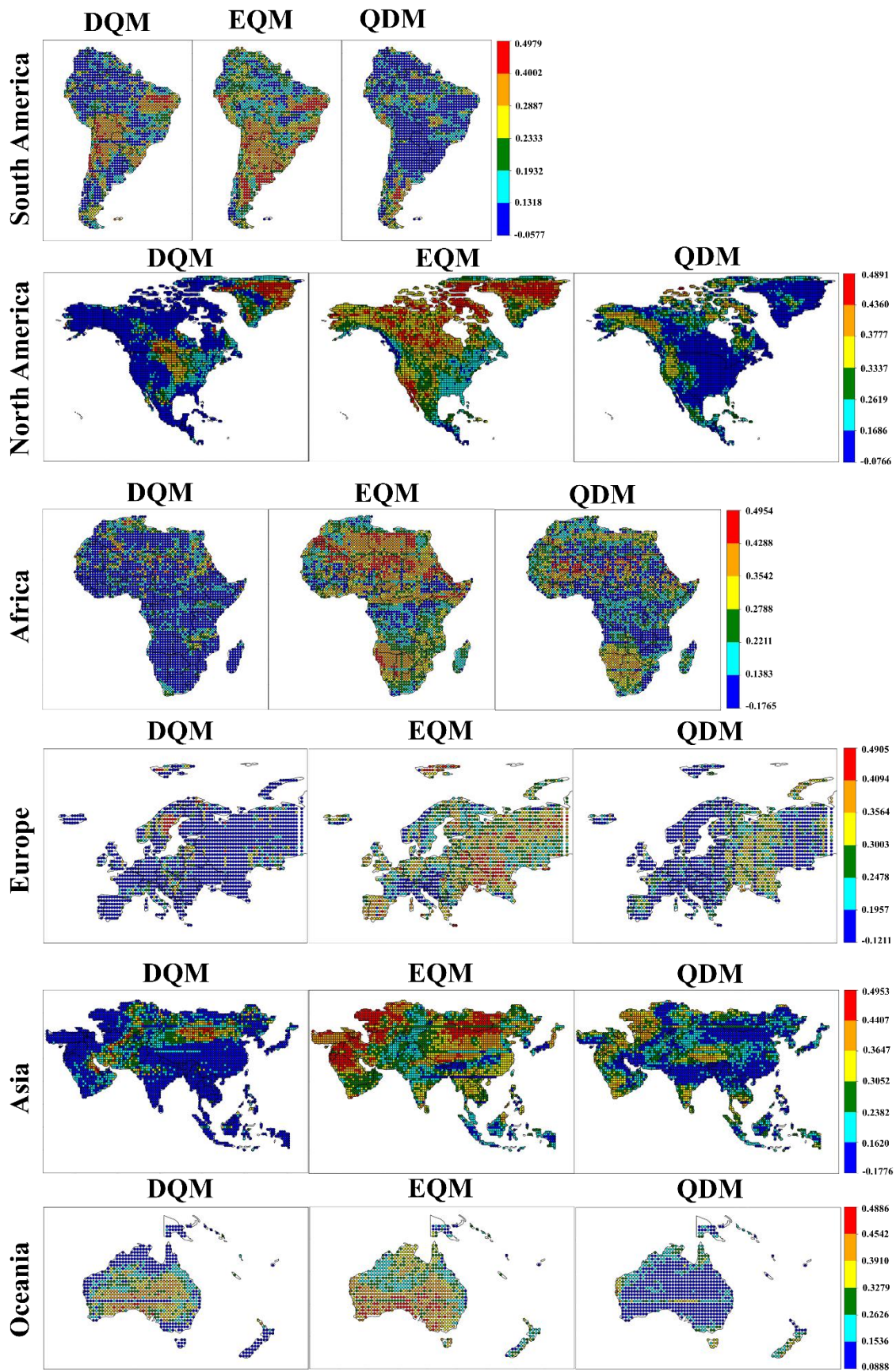
574 the comprehensive indices calculated by applying equal weights, weights that emphasize  
575 performance, and weights that emphasize uncertainty, respectively.

576 When equal weights were applied, EQM showed the highest CI across all continents. However,  
577 the index was lower in southern Europe and southeastern North America, but it calculated high  
578 values in most other regions. QDM showed high index values in some regions, although it was  
579 lower than EQM. For example, the CI results were high in the northern and western parts of  
580 North America and the central part of Europe. On the other hand, DQM was generally  
581 unsuitable in most regions but showed a relatively high index in Oceania.

582 When weights that emphasized performance were applied, DQM showed a high index in the  
583 central part of South America but low performance in most continents. Nevertheless, DQM  
584 showed a better index than QDM in some parts of Oceania. EQM showed the best index across  
585 most continents. While QDM was less suitable than EQM, it was still evaluated as a useful  
586 method in some continents.

587 Even when applying weights that increased the emphasis on uncertainty, similar results were  
588 obtained with the other weighting values. In particular, EQM was evaluated as the most suitable  
589 model across all continents, while DQM showed the opposite results.

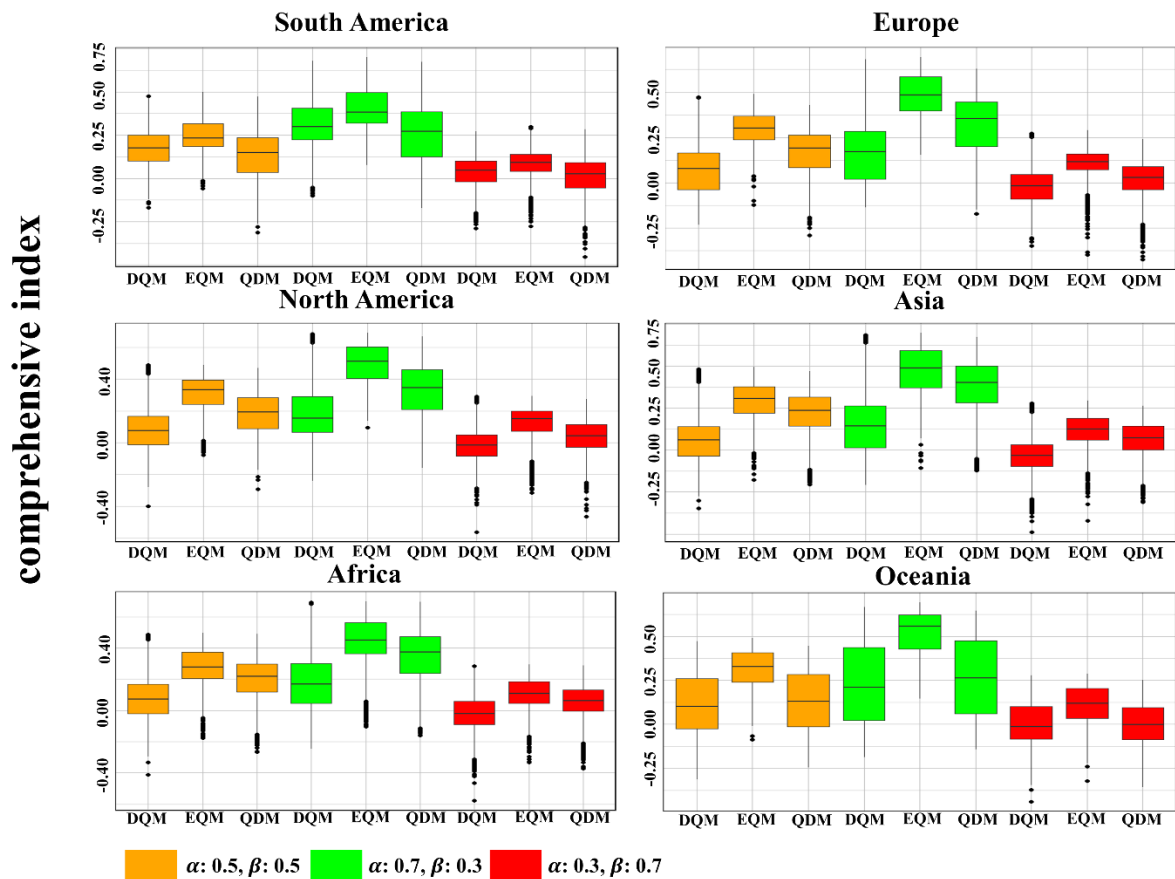
590



592 Figure 16. Spatial distribution of comprehensive indices for bias correction methods with equal  
 593 weights ( $\alpha: 0.5, \beta: 0.5$ ) across continents

594

595 Figure 17 presents a comparison of the comprehensive indices for three QM methods with  
 596 different weights for each continent using box plots. Overall, all methods showed absolutely  
 597 higher indices than the other weighting values in the values that emphasized more weight on  
 598 performance. In all weighted values, DQM showed the lowest indices in all continents except  
 599 for South America and Oceania, where it was slightly higher or similar to QDM. EQM showed  
 600 the best composite indices in all continents, outperforming both performance and uncertainty.  
 601 QDM showed high comprehensive indices in most continents, and the gap with EQM narrowed  
 602 significantly in the weighting values that emphasized performance more. Nevertheless, QDM  
 603 overall had lower comprehensive indices than EQM.  
 604



605

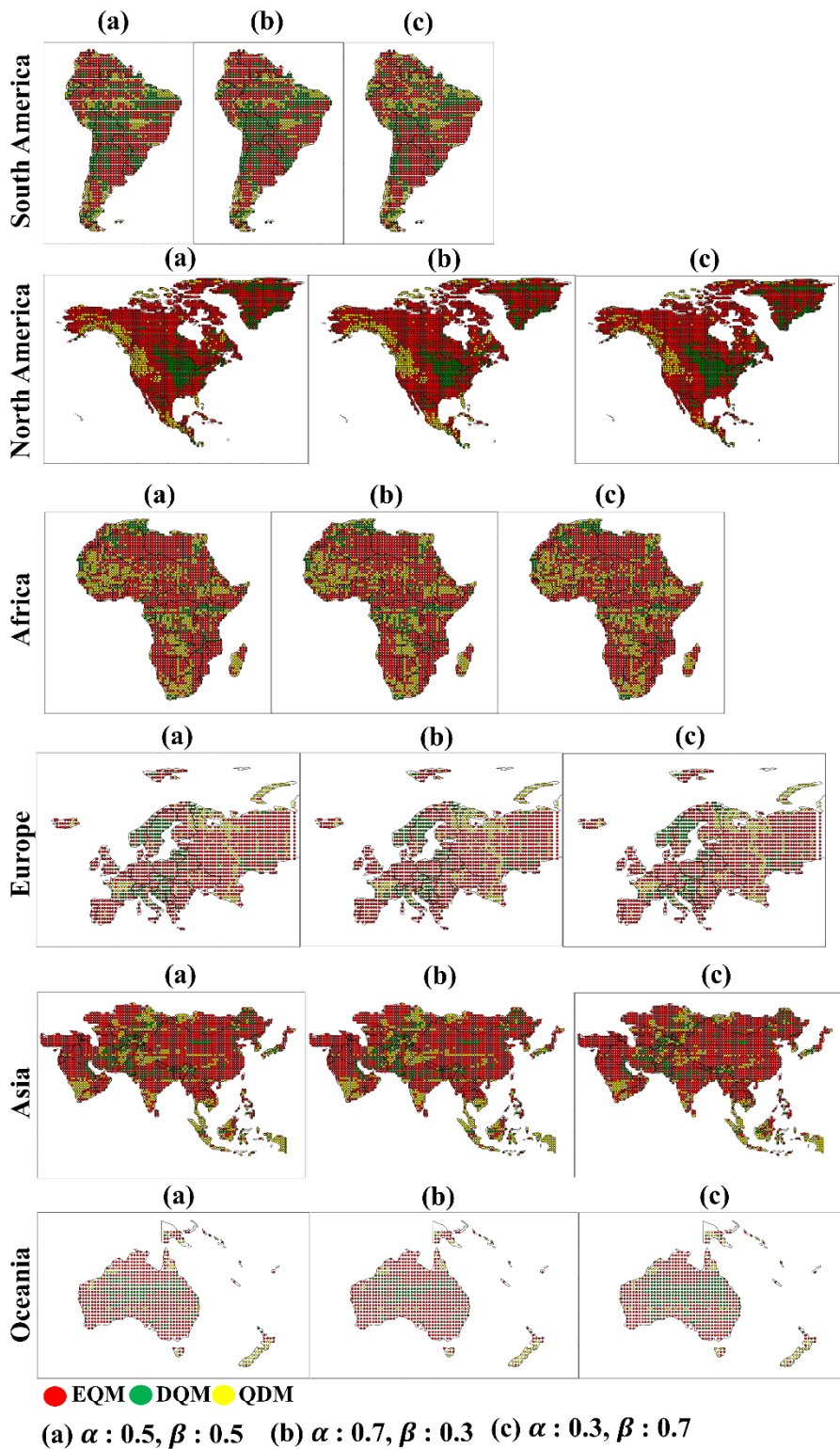
606 Figure 17. CI for three bias correction methods across continents with varying weights on  
 607 performance and uncertainty

608



609 **3.4.2 Selection of best bias correction method**

610 This study selected the best bias correction method for each continent based on the CI. Figure  
611 18 shows how the best bias correction method was selected for each continent by applying  
612 various weighting values of the CI. Overall, EQM was selected as the best correction method  
613 for most continents in all weighting values and was selected more than other methods in North  
614 America, Europe, Asia, and Oceania. DQM was selected the least in most continents except  
615 for South America and Oceania, and the number of selected grids tended to decrease as the  
616 weighting for uncertainty increased. QDM was selected as the proper bias correction method  
617 in western North America, southern and eastern Africa, and northern Europe. In addition, QDM  
618 was selected the most in Southeast Asia in all weighting values.



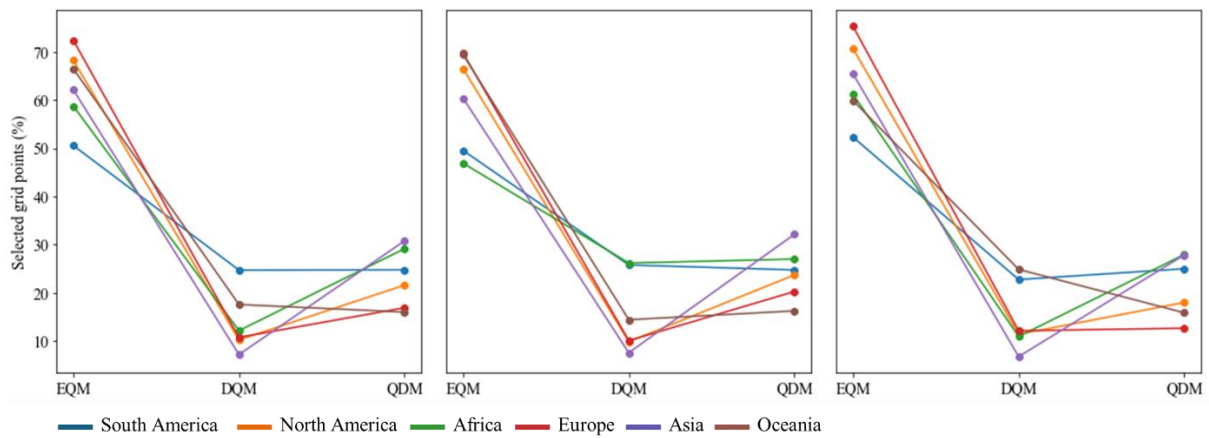
619

620 Figure 18. Selection of best bias correction methods across continents based on CI depending

621 on weighting values.

622

623 Figure 19 shows the number of selected grids for the best bias correction method across  
 624 continents based on three weighting values. Overall, EQM was the most frequently selected  
 625 method across all weighting values, demonstrating superior performance across all continents  
 626 compared to the other methods. Interestingly, as the weight for uncertainty increased, the  
 627 number of grids where EQM was selected also increased, while the number decreased as the  
 628 weight for performance increased. In contrast, QDM was chosen as the second-best method on  
 629 most continents, except for South America and Oceania. The number of selected grids for  
 630 QDM slightly increased as the performance weight increased. DQM was the least selected  
 631 method across most continents, indicating that it was the least suitable overall.  
 632



633  
 634 Figure 19. Ratios of selected grids for best bias correction methods across continents based on  
 635 different weighting values  
 636

#### 637 4. Discussion

638 Bias correction methods are widely used in correcting GCM outputs, and previous studies have  
 639 compared the performance of various methods (Homsí et al., 2019; Saranya and Vinish, 2021).  
 640 Among these, Quantile Mapping (QM) has consistently shown superior performance compared  
 641 to other methods, making it a widely used approach for bias correction. In particular, QDM,  
 642 EQM, and DQM, which are the focus of this study, are frequently employed in research  
 643 exploring and applying climate change projections based on GCM outputs (Cannon et al., 2015;  
 644 Switanek et al., 2016; Song et al., 2022a). Analyzing the strengths and limitations of these three  
 645 methods will provide valuable insights for climate researchers, enabling them to choose the  
 646 most suitable bias correction method for specific regions. In this context, this study further  
 647 evaluates the performance of QDM, EQM, and DQM, especially for daily precipitation, and

648 investigates how these methods perform across different regions. This section discusses the  
649 strengths and weaknesses of each method from various perspectives to provide a more balanced  
650 assessment.

651

#### 652 **4.1 Evaluation of bias correction methods performance**

653 The daily precipitation corrected by the three QM methods outperformed the raw GCM data  
654 (see Figure 1). All three methods showed strong overall performance, as indicated by the  
655 Taylor diagram, producing consistently good results across different regions. This highlights  
656 the need to use multiple performance metrics to fully understand the strengths and weaknesses  
657 of the three QM methods, as relying on a single analysis or macroscopic perspective can  
658 overlook important details. From this perspective, many studies have emphasized the  
659 application of a multifaceted analysis in selecting bias correction methods (Homsí et al., 2019;  
660 Cannon et al., 2015; Berg et al., 2022; Song et al., 2023). The spatial distribution of correction  
661 performance, as discussed in Section 3.1.2, varies significantly by continent. Figures 2 to 7  
662 reveal that the evaluated metrics differ across continents, underscoring the importance of  
663 region-specific correction methods. This finding aligns with Song et al. (2023), highlighting  
664 the importance of selecting appropriate correction methods based on the precipitation  
665 distribution at observation sites. Moreover, studies such as Homsí et al. (2019) and Saranya  
666 and Vinish (2021) also emphasize the variability in bias correction performance depending on  
667 the regional climate and data characteristics, reinforcing the need for tailored approaches. For  
668 example, the three QM methods tend to perform less effectively in regions with high  
669 precipitation, but their performance also varies by grid (e.g., southern India in Asia: RMSE;  
670 central Oceania: Pbias and EVS; central Europe: Pbias, MdAE, and KGE). While EQM  
671 performs well across most continents, DQM and QDM show superior results in specific regions.  
672 Similar results were made by Cannon et al. (2015), which highlighted differences in the  
673 performance of bias correction methods, particularly in handling extreme precipitation events.  
674 QDM's error-related metrics (South America: RMSE, MAE, and MSLE) are nearly identical  
675 to EQM's, yet QDM outperforms EQM regarding MdAE on more grids. These findings suggest  
676 that a more nuanced and detailed analysis of precipitation corrected by GCMs is necessary,  
677 aligning with the conclusions of Gudmundsson et al. (2012), which emphasize that the  
678 effectiveness of bias correction methods can vary significantly depending on local climate  
679 characteristics, highlighting the importance of selecting appropriate methods for each region.

680 These results suggest that a more detailed analysis of precipitation from corrected GCMs is  
681 needed.

682 This study compared the three QM methods for daily precipitation events above the 95th  
683 percentile (extreme precipitation) using the GEV distribution, as shown in Figure 10. The  
684 results indicate that DQM tends to correct more extreme precipitation events than QDM,  
685 aligning with previous findings that DQM captures a broader range of extremes. At the same  
686 time, QDM and EQM take a more conservative approach (as noted in previous studies such as  
687 Cannon et al., 2015). These findings suggest that EQM and QDM may be more suitable in  
688 regions vulnerable to floods and extreme weather events that require a more balanced and  
689 cautious approach. However, when comparing the differences in GEV distributions, there was  
690 no significant difference between methods in regions like Oceania and Europe (see Figure 9).  
691 These results imply that EQM can better handle extreme values or outliers in the data by  
692 directly comparing and correcting past and future distributions. In particular, EQM is consistent  
693 with previous studies in that it more accurately corrects observed distributions in non-stationary  
694 and highly variable climate variables, such as precipitation (Themeßl et al., 2012; Maraun,  
695 2013; Gudmundsson et al., 2012). Although there are significant advantages in observing the  
696 results of the correction method in detail from various perspectives, presenting these results  
697 without integrating them into a reasonable framework can increase confusion and uncertainty  
698 in climate change research (Wu et al., 2022). Therefore, it is essential to introduce a structured  
699 framework such as MCDA to provide a single integrated result.

700

#### 701 **4.2 Uncertainties of model and ensemble prediction in bias correction methods**

702 In climate modeling, quantifying uncertainty is essential to assess the reliability of bias-  
703 corrected precipitation data. This study applied BMA to quantify the uncertainty of three QM  
704 methods on a continental basis, addressing both model-specific and ensemble prediction  
705 uncertainties. Similar to the findings by Cannon et al. (2015), this analysis demonstrates how  
706 different bias correction methods yield varying uncertainty levels based on the underlying  
707 climate models. Notably, EQM showed the lowest weight variance across most continents,  
708 which means that the inter-model uncertainty for 11 GCMs corrected by EQM is lower than  
709 that of the other QM methods. The low uncertainty associated with EQM aligns with previous  
710 studies like Themeßl et al. (2012), which found that EQM consistently reduced discrepancies  
711 between modeled and observed data across regions. EQM's ability to manage extreme

712 precipitation and anomalous values based on observed distributions contributes to its reliability,  
713 a feature also emphasized by Gudmundsson et al. (2012). On the other hand, DQM showed the  
714 highest weight variance across all continents, indicating more significant uncertainty when  
715 applied to various GCMs. This uncertainty was particularly pronounced in regions with  
716 complex climate conditions, such as Southeast Asia, East Africa, and the Alps in Europe. These  
717 results align with Berg et al. (2022), who highlighted DQM's limitations in capturing long-term  
718 climate trends and extreme events. The higher uncertainty associated with DQM suggests that,  
719 while its detrending process is effective in correcting the mean, it may struggle in regions  
720 dominated by nonlinear climate patterns, as it does not sufficiently account for all quantiles in  
721 the distribution, particularly extremes, as noted by Cannon et al. (2015). QDM, though showing  
722 lower weight variance than DQM, still demonstrated higher uncertainty than EQM in regions  
723 with diverse climate characteristics. These results are consistent with the study of Tong et al.  
724 (2021), suggesting that QDM performs better under moderate precipitation scenarios. However,  
725 the uncertainty may increase under highly variable or extreme weather conditions. Furthermore,  
726 this study extended the uncertainty analysis to ensemble predictions, calculating the standard  
727 deviation of daily precipitation for each continent using BMA. The EQM-based ensemble  
728 consistently exhibited low standard deviations across all continents, indicating that EQM offers  
729 the most stable and reliable precipitation predictions. This finding echoes the conclusions  
730 drawn by Teng et al. (2015), where EQM provided more accurate and less uncertain projections.  
731 In contrast, DQM presented the most significant prediction uncertainty, reinforcing the need  
732 for caution when applying DQM in studies that require high-confidence data. These results  
733 emphasize the importance of weighing both performance and uncertainty when choosing a  
734 suitable bias correction method. EQM's consistent performance in reducing uncertainty across  
735 both model-specific and ensemble forecasts highlights its robustness as a preferred choice for  
736 climate research. However, the substantial uncertainty associated with DQM suggests that its  
737 use should be limited to regions where its detrending process can be beneficial. Overall, these  
738 findings stress the critical role of uncertainty quantification in climate change impact  
739 assessments and underscore the need for selecting bias correction methods based on a  
740 comprehensive evaluation of both performance and uncertainty.

741

#### 742 **4.3 Integrated assessment of bias correction methods**

743 This study selected the optimal QM method for each continent based on the CI, which considers  
744 uncertainty and performance. The critical point is that uncertainty is decisive when selecting a  
745 bias correction method. As shown in Figure 19, the optimal correction method varies depending  
746 on the continent, and the selected method also changes depending on the weight. These results  
747 suggest that uncertainty still exists, as Berg et al. (2022) pointed out, and that uncertainty must  
748 be considered when selecting the optimal method. In other words, even if the QM method has  
749 high performance, it is difficult to make a reasonable selection if the uncertainty contained in  
750 the method is significant. Overall, EQM showed the highest CI value in all continents, which  
751 means that it provides the most balanced results in terms of performance and uncertainty. These  
752 results are consistent with previous studies (Lafon et al., 2013; Teutschbein and Seibert, 2012;  
753 Teng et al., 2015) that showed high precipitation correction accuracy and excellent  
754 performance, especially under complex climate conditions. QDM was evaluated highly in some  
755 regions but performed worse than EQM overall. Berg et al. (2022) also pointed out that QDM  
756 is superior in general climate conditions but may perform worse in extreme climate situations,  
757 suggesting that this may increase the uncertainty of QDM in extreme climates. DQM was  
758 evaluated as an unsuitable method in most regions due to low CI values, which is consistent  
759 with the limitations of DQM mentioned in Cannon et al. (2015) and Berg et al. (2022). It was  
760 confirmed that DQM performs relatively well in dry climates but may perform worse in various  
761 climate conditions. In addition, some differences were observed with the results based on  
762 TOPSIS. For example, DQM was selected more than QDM in South America, but when the  
763 uncertainty weight was applied, QDM was selected more. Conversely, in Oceania, QDM was  
764 selected more than DQM, but when the uncertainty weight was increased to 0.7, DQM was  
765 selected more. These results are consistent with those of Lafferty and Srivier (2023), showing  
766 that when significant uncertainty exists, uncertainty can be greater despite high bias correction  
767 performance. In conclusion, EQM is the most balanced method regarding performance and  
768 uncertainty and will likely be preferred in future climate modeling studies. However, there may  
769 be more suitable QM methods depending on the region, and a comprehensive evaluation with  
770 various weights is needed. Therefore, when establishing climate change response strategies or  
771 policy decisions, it is essential to take a multifaceted approach that considers uncertainty  
772 together rather than relying on a single indicator or performance alone. It will enable more  
773 reliable predictions and better decision-making.

774

## 775 **5. Conclusion**

776 This study corrected and compared historical daily precipitation from 11 CMIP6 GCMs using  
777 three QM methods. Eleven statistical metrics were used to evaluate the performance of the  
778 precipitation corrected by three QM methods, and TOPSIS was applied to select performance-  
779 based priorities. BMA was applied to quantify model-specific and ensemble prediction  
780 uncertainties. Additionally, suitable QM methods were selected and compared using a CI that  
781 integrates TOPSIS performance scores with BMA uncertainty metrics. The conclusions of this  
782 study are as follows:

- 783 1. EQM showed the highest overall index across all continents, indicating that it provides  
784 the most balanced approach in terms of performance and uncertainty.
- 785 2. DQM effectively reproduced the dry climate in North Africa and parts of Central and  
786 Southwest Asia but showed the highest uncertainty across all continents. These results  
787 suggest that DQM may lose some long-term trend information, making it less reliable  
788 in regions prone to extreme weather events.
- 789 3. QDM performed better in certain regions, such as Southeast Asia, and was selected  
790 more often than DQM when uncertainty was given greater weight. QDM may be a  
791 promising alternative in areas where uncertainty plays a significant role.
- 792 4. Selecting an appropriate QM is required for high performance, and significant  
793 uncertainty can complicate rational decision-making. Therefore, a multifaceted  
794 approach considering performance and uncertainty is essential in climate modeling.

795 In conclusion, EQM has emerged as the preferred method due to its balanced performance, but  
796 this study emphasizes the importance of regional assessment and careful consideration of  
797 uncertainty when selecting a QM method. Future research should integrate greenhouse gas  
798 scenarios to improve the accuracy of climate predictions and provide a more comprehensive  
799 understanding of future climate risks.

800

### 801 **Code availability**

802 Codes for benchmarking the xclim of python package are available from  
803 <https://doi.org/10.5281/zenodo.10685050> (Bourgault et al., 2024). Furthermore, the CI  
804 proposed in this study, along with the TOPSIS and BMA used within it, is available at  
805 <https://doi.org/10.5281/zenodo.14351816> (Song, 2024b).

806



807 **Data availability**

808 The data used in this study are publicly available from multiple sources. CMIP6 General  
809 Circulation Models (GCMs) outputs were obtained from the Earth System Grid Federation  
810 (ESGF) data portal at <https://esgf-node.llnl.gov/search/cmip6/>. Users can select data types such  
811 as climate variables, time series, and experiment ID, which can be downloaded as NC files.  
812 Furthermore, CMIP6 GCMs output can also be accessed in Eyring et al. (2016) The ERA5  
813 reanalysis dataset used in this study is available through the Copernicus Data Store (CDS)  
814 provided by ECMWF ([https://cds.climate.copernicus.eu/cdsapp#!/dataset/reanalysis-era5-  
815 single-levels?tab=overview](https://cds.climate.copernicus.eu/cdsapp#!/dataset/reanalysis-era5-single-levels?tab=overview)). ERA5 is available at <https://doi.org/10.24381/cds.bd0915c6>  
816 (Hersbach et al., 2023). The daily precipitation datasets from CMIP6 GCM and ERA5 used in  
817 this study are available at <https://doi.org/10.6084/m9.figshare.27999167.v5> (Song, 2024c).

818  
819 **Author contributions**

820 Young Hoon Song: Conceptualization, Methodology, Data curation, Funding acquisition,  
821 Visualization, Writing – original draft, Writing – review & editing. Eun Sung Chung: Formal  
822 analysis, Funding acquisition, Methodology, Project administration, Supervision, Validation,  
823 Writing-review & editing

824  
825 **Declaration of Competing Interests**

826 The authors declare that they have no known competing financial interests or personal  
827 relationships that could have appeared to influence the work reported in this paper.

828  
829 **Acknowledgement**

830 This study was supported by National Research Foundation of Korea (NRF) (RS-2023-  
831 00246767\_2; 2021R1A2C200569914)

832  
833 **Reference**

- 834 1. Abdelmoaty, H.M., and Papalexiou, S.M.: Changes of Extreme Precipitation in  
835 CMIP6 Projections: Should We Use Stationary or Nonstationary Models? *J. Clim.*  
836 36(9), 2999-3014, <https://doi.org/10.1175/JCLI-D-22-0467.1>, 2023.
- 837 2. Ansari, R., Casanueva, A., Liaqat, M.U., and Grossi, G.: Evaluation of bias  
838 correction methods for a multivariate drought index: case study of the Upper Jhelum

- 839 Basin. *GMD* 16(7), 2055-2076, <https://doi.org/10.5194/gmd-16-2055-2023>, 2023.
- 840 3. Berg P., Bosshard, T., Yang, W., and Zimmermann, K.: MIdASv0.2.1 – Multi-scale  
841 bias AdjStment. *GMD* 15, 6165-6180, <https://doi.org/10.5194/gmd-15-6165-2022>,  
842 2022
- 843 4. Bourgault, P., Huard, D., Smith, T.J., Logan, T., Aoun, A., Lavoie, J., Dupuis, É.,  
844 Rondeau-Genesse, G., Alegre, R., Barnes, C., Beaupré Laperrière, A., Biner, S.,  
845 Caron, D., Ehbrecht, C., Fyke, J., Keel, T., Labonté, M.P., Lierhammer, L., Low,  
846 J.F., Quinn, J., Roy, P., Squire, D., Stephens, Ag., Tanguy, M., Whelan, C., Braun,  
847 M., Castro, D.: *xclim: xarray-based climate data analytics (0.48.1)*. Zenodo [Code],  
848 <https://doi.org/10.5281/zenodo.10685050>, 2024.
- 849 5. Cannon, A. J., Sobie, S. R., and Murdock, T.Q.: Bias correction of GCM  
850 precipitation by quantile mapping: How well do methods preserve changes in  
851 quantiles and extremes? *J. Clim.* 28(17), 6938-6959, [https://doi.org/10.1175/JCLI-D-](https://doi.org/10.1175/JCLI-D-14-00754.1)  
852 14-00754.1, 2015.
- 853 6. Cannon, A.J.: Multivariate quantile mapping bias correction: an N-dimensional  
854 probability density function transform for climate model simulations of multiple  
855 variables. *Clim. Dyn.* 50, 31–49. <https://doi.org/10.1007/s00382-017-3580-6>, 2018.
- 856 7. Chae, S. T., Chung, E. S., and Jiang, J.: Robust siting of permeable pavement in  
857 highly urbanized watersheds considering climate change using a combination of  
858 fuzzy-TOPSIS and the VIKOR method. *Water Resour. Manag.* 36(3), 951–969,  
859 <https://doi.org/10.1007/s11269-022-03062-y>, 2022.
- 860 8. Chua, Z.W., Kuleshov, Y., Watkins, A.B., Choy, S., and Sun, C.: A Comparison of  
861 Various Correction and Blending Techniques for Creating an Improved Satellite-  
862 Gauge Rainfall Dataset over Australia. *Remote Sens.* 14(2), 261,  
863 <https://doi.org/10.3390/rs14020261>, 2022.
- 864 9. Chung, E. S., and Kim, Y.J.: Development of fuzzy multi-criteria approach to  
865 prioritize locations of treated wastewater use considering climate change scenarios.  
866 *JEM* 146, 505–516, <https://doi.org/10.1016/j.jenvman.2014.08.013>, 2014.
- 867 10. Cox, P., and Stephenson, D.: A changing climate for prediction. *Science* 317(5835),  
868 207–208, <https://www.science.org/doi/10.1126/science.1145956>, 2007.
- 869 11. Deser, C., Phillips, A., Bourdette, V., and Teng, H.: Uncertainty in climate change  
870 projections: the role of internal variability. *Clim. Dyn.* 38, 527–546,

- 871 <https://doi.org/10.1007/s00382-010-0977-x>, 2012
- 872 12. Déqué, M.: Frequency of precipitation and temperature extremes over France in an  
873 anthropogenic scenario: Model results and statistical correction according to  
874 observed values. *Glob. Planet. Change.* 57(1-2), 16-26,  
875 <https://doi.org/10.1016/j.gloplacha.2006.11.030>, 2007.
- 876 13. Ehret, U., Zehe, E., Wulfmeyer, V., Warrach-Sagi, K., and Liebert, J.: HESS  
877 Opinions "Should we apply bias correction to global and regional climate model  
878 data?". *HESS* 16(9), 3391-3404, <https://doi.org/10.5194/hess-16-3391-2012>, 2012.
- 879 14. Enayati, M., Bozorg-Haddad, O., Bazrafshan, J., Hejabi, S., and Chu, X.: Bias  
880 correction capabilities of quantile mapping methods for rainfall and temperature  
881 variables. *Water and Climate change* 12(2), 401-419,  
882 <https://doi.org/10.2166/wcc.2020.261>, 2021.
- 883 15. Evin, G., Ribes, A., and Corre, L.: Assessing CMIP6 uncertainties at global warming  
884 levels. *Clim Dyn.* <https://doi.org/10.1007/s00382-024-07323-x>, 2024.
- 885 16. Eyring, V., Bony, S., Meehl, G., Senior, C., Stevens, B., Stouffer, R., and Taylor, K.:  
886 **Overview of the Coupled Model Intercomparison Project Phase 6 (CMIP6)**  
887 **experimental design and organization. *Geoscientific Model Development*, 9(5),**  
888 **1937–1958. 2016. <https://doi.org/10.5194/gmd-9-1937-2016>**
- 889 17. Galton, F.: Regression Towards Mediocrity in Hereditary Stature. *The Journal of the*  
890 *Anthropological Institute of Great Britain and Ireland* 15, 246-263,  
891 <https://doi.org/10.2307/2841583>, 1886.
- 892 18. Giorgi, F., and Mearns, L.O.: Calculation of average, uncertainty range, and  
893 reliability of regional climate changes from AOGCM simulations via the “reliability  
894 ensemble averaging” (REA) method, *J. Clim.* 15, 1141–1158,  
895 [https://doi.org/10.1175/1520-0442\(2002\)015<1141:COAURA>2.0.CO;2](https://doi.org/10.1175/1520-0442(2002)015<1141:COAURA>2.0.CO;2), 2000.
- 896 19. Gupta, H.V., Kling, H., Yilmaz, K.K., and Martinez, G.F.: Decomposition of the  
897 mean squared error and NSE performance criteria: Implications for improving  
898 hydrological modelling. *J. Hydrol.* 377(1–2), 80–91,  
899 <https://doi.org/10.1016/j.jhydrol.2009.08.003>, 2009
- 900 20. Gudmundsson, L., Bremnes, J.B., Haugen, J.E., and Engen-Skaugen, T.: Technical  
901 Note: Downscaling RCM precipitation to the station scale using statistical  
902 transformations – a comparison of methods. *HESS* 16(9), 3383–3390,

- 903 <https://doi.org/10.5194/hess-16-3383-2012>, 2012.
- 904 21. Hamed, M.M., Nashwan, M.S., Shahid, S., Wang, X.J., Ismail, T.B., Dewan, A., and  
905 Asaduzzaman, M.d: Future Köppen-Geiger climate zones over Southeast Asia using  
906 CMIP6 Multimodel Ensemble. *Atmos. Res.* 283(1), 106560,  
907 <https://doi.org/10.1016/j.atmosres.2022.106560>, 2023.
- 908 22. Hersbach, H., Bell, B., Berrisford, P., Hirahara, S., Horányi, A., Muñoz-Sabater, J.,  
909 Nicolas, J., Peubey, C., Radu, R., Schepers, D., Simmons, A., Soci, C., Abdalla, S.,  
910 Abellan, X., Balsamo, G., Bechtold, P., Biavati, G., Bidlot, J., Bonavita, M., Chiara,  
911 G., Dahlgren, P., Dee, D., Diamantakis, M., Dragani, R., Flemming, J., Forbes, R.,  
912 Fuentes, M., Geer, A., Haimberger, L., Healy, S., Hogan, R. J., Hólm, E., Janisková,  
913 M., Keeley, S., Laloyaux, P., Lopez, P., Lupu, C., Radnoti, G., Rosnay, P., Rozum,  
914 I., Vamborg, F., Villaume, S., and Thépaut, J.: The ERA5 global reanalysis, *Q. J.*  
915 *Roy. Meteor. Soc.*, 146, 1999–2049, <https://doi.org/10.1002/qj.3803>, 2020.
- 916 23. Hersbach, H., Bell, B., Berrisford, P., Biavati, G., Horányi, A., Muñoz Sabater, J.,  
917 Nicolas, J., Peubey, C., Radu, R., Rozum, I., Schepers, D., Simmons, A., Soci, C.,  
918 Dee, D., and Thépaut, J.-N.: ERA5 hourly data on pressure levels from 1940 to  
919 present, Copernicus Climate Change Service (C3S) Climate Data Store (CDS),  
920 <https://doi.org/10.24381/cds.bd0915c6>, 2023.
- 921 24. Homsí, R., Shiru, M. S., Shahid, S., Ismail, T., Harun, S. B., Al-Ansari, N., and  
922 Yaseen, Z.M: Precipitation projection using a CMIP5 GCM ensemble model: a  
923 regional investigation of Syria. *Eng. Appl. Comput. Fluid Mech.* 14(1), 90–106,  
924 <https://doi.org/10.1080/19942060.2019.1683076>, 2019.
- 925 25. Hoeting J.A., Madigan D., Raftery A.E., and Volinsky C.T.: Bayesian model  
926 averaging: A tutorial (with discussion). *Stat. Sci.* 214, 382-417,  
927 <https://doi.org/10.1214/ss/1009212519>, 1999.
- 928 26. Hosking, J.R.M., Wallis, J.R., and Wood, E.F.: Estimation of the generalized  
929 extreme value distribution by the method of probability weighted moments.  
930 *Technometrics* 27, 251–261, <https://doi.org/10.1080/00401706.1985.10488049>,  
931 1985.
- 932 27. Hosking, J.R.M.: L-moments: Analysis and estimation of distributions using linear  
933 combinations of order statistics. *J. R. Stat.* 52, 105–124,  
934 <https://doi.org/10.1111/j.2517-6161.1990.tb01775.x>, 1990.

- 935 28. Hwang, C. L., and Yoon, K.: Multiple attribute decision making: Methods and  
936 applications. Springer-Verlag. <https://doi.org/10.1007/978-3-642-48318-9>. 1981.
- 937 29. IPCC: Climate Change 2021: The Physical Science Basis. Contribution of Working  
938 Group I to the Sixth Assessment Report of the Intergovernmental Panel on Climate  
939 Change, edited by: Masson-Delmotte, V., Zhai, P., Pirani, A., Connors, S. L., Péan,  
940 C., Berger, S., Caud, N., Chen, Y., Goldfarb, L., Gomis, M. I., Huang, M., Leitzell,  
941 K., Lonnoy, E., Matthews, J. B. R., Maycock, T. K., Waterfield, T., Yelekçi, O., Yu,  
942 R., and Zhou, B., Cambridge University Press,  
943 <https://doi.org/10.1017/9781009157896>, 2021.
- 944 30. IPCC: Climate Change 2022: Impacts, Adaptation, and Vulnerability. Contribution  
945 of Working Group II to the Sixth Assessment Report of the Intergovernmental Panel  
946 on Climate Change, edited by: Pörtner, H.-O., Roberts, D. C., Tignor, M.,  
947 Poloczanska, E. S., Mintenbeck, K., Alegría, A., Craig, M., Langsdorf, S., Lösschke,  
948 S., Möller, V., Okem, A., and Rama, B., Cambridge University Press,  
949 <https://doi.org/10.1017/9781009325844>, 2022.
- 950 31. Ishizaki, N.N., Shiogama, H., Hanasaki, N., Takahashi, K., and Nakaegawa, T.:  
951 Evaluation of the spatial characteristics of climate scenarios based on statistical and  
952 dynamical downscaling for impact assessments in Japan. *Int. J. Climatol.* 43(2),  
953 1179-1192, <https://doi.org/10.1002/joc.7903>, 2022.
- 954 32. Jobst, A.M., Kingston, D.G., Cullen, N.J., and Schmid, J.: Intercomparison of  
955 different uncertainty sources in hydrological climate change projections for an alpine  
956 catchment (upper Clutha River, New Zealand). *HESS* 22, 3125-3142,  
957 <https://doi.org/10.5194/hess-22-3125-2018>, 2018.
- 958 33. Lafferty, D.C., and Sriver, R.L.: Downscaling and bias-correction contribute  
959 considerable uncertainty to local climate projections in CMIP6. *npj Clim Atmos*  
960 *Sci* 6, 158, <https://doi.org/10.1038/s41612-023-00486-0>, 2023.
- 961 34. Lafon, T., Dadson, S., Buys, G., and Prudhomme, C.: Bias correction of daily  
962 precipitation simulated by a regional climate model: a comparison of methods. *Int. J.*  
963 *Climatol.* 33, 1367-1381, <http://dx.doi.org/10.1002/joc.3518>, 2013.
- 964 35. Lin, J.: Divergence measures based on the Shannon entropy. *IEEE Transactions on*  
965 *Information Theory* 37(1), 145–151, <https://doi.org/10.1109/18.61115>, 1991.
- 966 36. Maraun, D.: Bias correction, quantile mapping, and downscaling: Revisiting the

- 967 inflation issue. *J. Clim.* 26(6), 2137-2143, [https://doi.org/10.1175/JCLI-D-12-](https://doi.org/10.1175/JCLI-D-12-00821.1)  
968 00821.1, 2013.
- 969 37. Nair, M.M.A., Rajesh, N., Sahai, A.K., and Lakshmi Kumar, T.V.: Quantification of  
970 uncertainties in projections of extreme daily precipitation simulated by CMIP6  
971 GCMs over homogeneous regions of India. *Int. J. Climatol.* 43(15), 7365-7380,  
972 <https://doi.org/10.1002/joc.8269>, 2023.
- 973 38. Nash, J.E., and Sutcliffe, J.V.: River flow forecasting through conceptual models part  
974 I—A discussion of principles. *J. Hydrol.* 10, 282–290, [https://doi.org/10.1016/0022-](https://doi.org/10.1016/0022-1694(70)90255-6)  
975 1694(70)90255-6Return to ref 1970 in article, 1970.
- 976 39. Pathak, R., Dasari, H.P., Ashok, K., and Hoteit, I., Effects of multi-observations  
977 uncertainty and models similarity on climate change projections. *npj clim. atmos. sci.*  
978 6, 144, <https://doi.org/10.1038/s41612-023-00473-5>, 2023.
- 979 40. Piani, C., Weedon, G. P., Best, M., Gomes, S. M., Viterbo, P., Hagemann, S., and  
980 Haerter, J.O.: Statistical bias correction of global simulated daily precipitation and  
981 temperature for the application of hydrological models. *J. Hydrol.* 395(3-4), 199-215,  
982 <https://doi.org/10.1016/j.jhydrol.2010.10.024>, 2010.
- 983 41. Rahimi, R., Tavakol-Davani, H., and Nasser, M.: An Uncertainty-Based Regional  
984 Comparative Analysis on the Performance of Different Bias Correction Methods in  
985 Statistical Downscaling of Precipitation. *Water Resour. Manag.* 35, 2503–2518,  
986 <https://doi.org/10.1007/s11269-021-02844-0>, 2021.
- 987 42. Rajulapati, C.R., and Papalexiou, S.M.: Precipitation Bias Correction: A Novel  
988 Semi-parametric Quantile Mapping Method. *Earth Space Sci.* 10(4),  
989 e2023EA002823, <https://doi.org/10.1029/2023EA002823>, 2023.
- 990 43. Saranya, M.S., and Vinish, V.N.: Evaluation and selection of CORDEX-SA datasets  
991 and bias correction methods for a hydrological impact study in a humid tropical river  
992 basin, Kerala. *Water Climate Change* 12(8), 3688-3713,  
993 <https://doi.org/10.2166/wcc.2021.139>, 2021.
- 994 44. Shanmugam, M., Lim, S., Hosan, M.L. Shrestha, S., Babel, M.S., and Viridis, S.G.P.:  
995 Lapse rate-adjusted bias correction for CMIP6 GCM precipitation data: An  
996 application to the Monsoon Asia Region. *Environ Monit Assess.* 196, 49,  
997 <https://doi.org/10.1007/s10661-023-12187-5>, 2024.
- 998 45. Song, J. Y., and Chung, E.S.: Robustness, uncertainty, and sensitivity analyses of

- 999 TOPSIS method to climate change vulnerability: Case of flood damage. *Water*  
1000 *Resour. Manag.*, 30(13), 4751–4771, <https://doi.org/10.1007/s11269-016-1451-2>,  
1001 2016.
- 1002 46. Song, Y.H., Shahid, S., and Chung, E.S.: Differences in multi-model ensembles of  
1003 CMIP5 and CMIP6 projections for future droughts in South Korea. *Int. J. Climatol.*  
1004 42(5), 2688-2716, <https://doi.org/10.1002/joc.7386>, 2022a.
- 1005 47. Song, Y.H., Chung, E.S., and Shahid, S.: The New Bias Correction Method for Daily  
1006 Extremes Precipitation over South Korea using CMIP6 GCMs. *Water Resour.*  
1007 *Manag.* 36, 5977–5997, <https://doi.org/10.1007/s11269-022-03338-3>, 2022b.
- 1008 48. Song, Y.H., Chung, E.S., and Shahid, S.: Uncertainties in evapotranspiration  
1009 projections associated with estimation methods and CMIP6 GCMs for South Korea.  
1010 *Sci. Total Environ.* 825, 153953, <https://doi.org/10.1016/j.scitotenv.2022.153953>,  
1011 2023.
- 1012 49. Song, Y.H., Chung, E.S., and Shahid, S.: Global Future Climate Signal by Latitudes  
1013 Using CMIP6 GCMs. *Earths Future* 12(3), e2022EF003183,  
1014 <https://doi.org/10.1029/2022EF003183>, 2024a.
- 1015 50. Song, Y.H.: *Comprehensive Index and Performance-Related Code, Zenodo [Code]*,  
1016 <https://zenodo.org/records/14351816>. 2024b
- 1017 51. Song, Y.H.: *Historical Daily Precipitation Data of CMIP6 GCMs and ERA5,*  
1018 *Figshare [Dataset]*, <https://doi.org/10.6084/m9.figshare.27999167.v5>. 2024c
- 1019 52. Switanek, M.B., Troch, P.A., Castro, C.L., Leuprecht, A., Chang, H.I., Mukherjee,  
1020 R., and Demaria E.M.C.: Scaled distribution mapping: a bias correction method that  
1021 preserves raw climate model projected changes. *HESS* 21(6), 2649-2666,  
1022 <https://doi.org/10.5194/hess-21-2649-2017>, 2017.
- 1023 53. Tanimu, B., Bello, AA.D., Abdullahi, S.A. Ajibike, M.A., Yaseen, Z.M.,  
1024 Kamruzzaman, M., Muhammad, M.K.I., and Shahid, S.: Comparison of conventional  
1025 and machine learning methods for bias correcting CMIP6 rainfall and temperature in  
1026 Nigeria. *Theor. Appl. Climatol.* 155, 4423–4452, [https://doi.org/10.1007/s00704-](https://doi.org/10.1007/s00704-024-04888-9)  
1027 024-04888-9, 2024.
- 1028 54. Teutschbein, C., AND Seibert, J.: Bias correction of regional climate model  
1029 simulations for 575 hydrological climate-change impact studies: Review and  
1030 evaluation of different 576 methods. *J. Hydrol.* 16, 12-29,

- 1031 <http://dx.doi.org/10.1016/j.jhydrol.2012.05.052>, 2012.
- 1032 55. Teng, J., Potter, N. J., Chiew, F. H. S., Zhang, L., Wang, B., Vaze, J., and Evans,  
1033 J.P.: 2015. How does bias correction of regional climate model precipitation affect  
1034 modelled runoff? *HESS* 19, 711–728, <https://doi.org/10.5194/hess-19-711-2015>,  
1035 2015.
- 1036 56. Themeßl, M.J., Gobiet, A., and Heinrich, G.: Empirical-statistical downscaling and  
1037 error correction of daily precipitation from regional climate models. *Int. J. Climatol.*  
1038 31(10), 1530-1544, <https://doi.org/10.1002/joc.2168>, 2012.
- 1039 57. Tong, Y., Gao, X., Han, Z., Xu, Y., and Giorgi, F.: Bias correction of temperature  
1040 and precipitation over China for RCM simulations using the QM and QDM methods.  
1041 *Clim. Dyn.* 57, 1425-1443, <https://doi.org/10.1007/s00382-020-05447-4>, 2021.
- 1042 58. Yip, S., Ferro, C.A.T., Stephenson, D.B., and Hawkins, E.: A simple, coherent  
1043 framework for partitioning uncertainty in climate predictions. *J. Clim.* 24(17), 4634–  
1044 4643, <https://doi.org/10.1175/2011JCLI4085.1>, 2011.
- 1045 59. Woldemeskel, F. M., Sharma, A. Sivakumar, B., and Mehrotra, R.: A framework to  
1046 quantify GCM uncertainties for use in impact assessment studies. *J. Clim.* 519,  
1047 1453–1465, <https://doi.org/10.1016/j.jhydrol.2014.09.025>, 2014.
- 1048 60. Wu, Y., Miao, C., Fan, X., Gou, J., Zhang, Q., and Zheng, H.: Quantifying the  
1049 uncertainty sources of future climate projections and narrowing uncertainties with  
1050 Bias Correction Techniques. *Earths Future*, 10(11), e2022EF002963, 2022.
- 1051 61. Zhang, S., Zhou, Z., Peng, P., and Xu, C.: A New Framework for Estimating and  
1052 Decomposing the Uncertainty of Climate Projections. *J. Clim.* 37(2), 365-384,  
1053 <https://doi.org/10.1175/JCLI-D-23-0064.1>, 2024.
- 1054